Gondwana Research 56 (2018) 119–134

Contents lists available at ScienceDirect

Gondwana Research

journal homepage: www.elsevier.com/locate/gr

Variability of orogenic magmatism during Mediterranean-style continental collisions: A numerical modelling approach

N. Andrić [a,b,*], K. Vogt [a], L. Matenco [a], V. Cvetković [b], S. Cloetingh [a], T. Gerya [c]

[a] Utrecht University, Faculty of Geosciences, Utrecht, The Netherlands
[b] University of Belgrade, Faculty of Mining and Geology, Belgrade, Serbia
[c] Department of Earth Sciences, ETH-Zurich, Sonneggstrasse 5, 8092 Zurich, Switzerland

ARTICLE INFO

Article history:
Received 20 April 2017
Received in revised form 18 November 2017
Accepted 21 December 2017
Available online 4 January 2018

Handling Editor: N. Rawlinson

Keywords:
Collision
Magmatism
Numerical modelling
Dinarides
Mediterranean orogens

ABSTRACT

The relationship between magma generation and the tectonic evolution of orogens during subduction and subsequent collision requires self-consistent numerical modelling approaches predicting volumes and compositions of the produced magmatic rocks. Here, we use a 2D magmatic-thermomechanical numerical modelling procedure to analyse rapid subduction of a narrow ocean, followed by Mediterranean style collision, which is characterized by the gradual accretion of lower plate material and slab migration towards the orogenic foreland. Our results suggest that magmatism has a large-scale geodynamic effect by focusing deformation throughout the entire subduction and collision process. The rheological structure and compositional layering of the crust impose a key control on the distribution of magmatic rocks within the orogen. Compared to previous simplified homogeneous crustal models, a compositionally layered crust causes an increase in felsic material influx during continental collision and results in shallower magmatic sources that migrate with time towards the foreland. Changes in the deformation style may be locally driven by magma emplacement rather than by slab movement. Our modelling also demonstrates that the migration pattern of the deformation front and the magmatic arc relative to the location of the suture zone may be driven by lower crustal indentation in the overriding plate during early stages of collision. The modelling predicts a gradual change in magma source composition with time from typical calc-alkaline to ones associated with relamination and eduction during subduction, collision and slab detachment. This transition explains the compositional changes of magma their temporal and spatial migration, as well as the observed link with deformation in the Dinarides orogen of Central Europe selected as a case study.

1. Introduction

The mechanics of continental collision have been analysed in numerous analogue and numerical studies that have revealed the critical influence of several key parameters on orogenic build-up, such as the rheology of the continental lithosphere, the thermal age of the subducting oceanic lithosphere, the convergence rate and external forcing factors, such as the rate of erosion and/or sedimentation (e.g., Burov and Yamato, 2008; Ueda et al., 2012; Willingshofer et al., 2013; Erdős et al., 2014 and references therein). Most of these studies have focused on the mechanical growth of orogens, which is influenced by a number of processes, such as continental subduction (e.g., Pysklywec et al., 2002; Pysklywec et al., 2010; Gray and Pysklywec, 2010; Vogt et al., 2017ab), delamination of continental lithosphere (e.g., Ueda et al., 2012), crustal relamination (e.g., Hacker et al., 2011), slab detachment (e.g., Duretz et al., 2011), eduction (e.g., Andersen et al., 1991; Duretz and Gerya, 2013) or exhumation of continental crust (e.g., Brun and Faccenna, 2008; Beaumont et al., 2009; Sizova et al., 2012). Many collisional systems reveal changes in magmatism in terms of volume, composition, spatial and temporal distribution (e.g., Pearce et al., 1990; Duggen et al., 2008; Lustrino and Wilson, 2007; Neill et al., 2015; Menant et al., 2016a). Previous numerical studies have analysed the compositional change and production rate of magmas and showed that the mechanics of subduction and subsequent collision control their location, composition and emplacement mechanism (e.g., Dymkova et al., 2016; Menant et al., 2016b). Magma production and emplacement was, moreover shown to lower lithospheric strength and to control lithospheric deformation (e.g., Faccenda et al., 2009; Gerya and Meilick, 2011; Gerya et al., 2015).

Observations have shown that a number of Mediterranean collisional orogens, such as the Apennines, Carpathians, Betics-Rif or Dinarides, show crustal accretion of lower plate material, slab retreat as well as an overall migration pattern of deformation and magmatism towards the orogenic foreland with time (e.g., Royden, 1993; Picotti and Pazzaglia, 2008; Matenco et al., 2010; Schefer et al., 2011; Vergés and Fernàndez, 2012; Faccenna et al., 2013; Göğüş et al., 2016). Modelling

* Corresponding author at: Utrecht University, Department of Earth Sciences, PO Box: 80021, 3508TA Utrecht, The Netherlands.
E-mail address: n.andric@uu.nl (N. Andrić).

https://doi.org/10.1016/j.gr.2017.12.007
1342-937X/

studies have shown that crustal accretion and migration of deformation is driven by rheological contrasts, associated with continental subduction and slab-retreat (Willingshofer and Sokoutis, 2009; Vogt et al., 2017a, 2017b), but the overall variability of magmatism during this process has not been addressed. Observations in the Mediterranean orogens associated with a migration of crustal accretion have shown that the foreland directed migration of magmatism is associated with a geochemical variability from predominantly mafic to predominantly felsic, and it is generally explained to be driven by the slab retreat in the Apennines, Dinarides or Carpathians (e.g., Seghedi et al., 2004; Duggen et al., 2005; Dilek and Altunkaynak, 2009; Lustrino et al., 2011; Cvetković et al., 2013; Menant et al., 2016a).

In this overall context, the continental collision processes driving the magmatic diversity found in these Mediterranean orogens is still not understood and is difficult to quantify solely by conventional field studies and geochemical techniques. Hence, self-consistent numerical approaches, which are able to quantify the temporal and spatial generation of melts during subduction and collision, offer an important additional tool to address complex interactions between magma production and lithospheric scale processes.

In this study, we present a series of 2D magmatic-thermomechanical experiments designed to quantitatively couple subduction and collision with magma generation, focusing on its compositional changes. Our setup is designed to simulate rapid subduction of a narrow ocean, followed by continental collision. By starting from a reference model, we further perform a parametric analysis on the role of crustal rheology, ocean size and thermal age, and convergence rate. The results are compared with one of the above mentioned Mediterranean orogens, the Dinarides Mountains of Central Europe, which were affected by subduction, collision and back-arc extension, and have a well-preserved record of temporal and spatial changes in magma composition.

2. Numerical modelling methodology

Our magmatic-thermomechanical model is based on the i2vis Code and solves a series of thermal and mechanical equations by combing a finite difference approach and a marker in cell technique (Gerya and Yuen, 2003a, 2003b, see also Appendix 1, Tables 1 and 2). The model incorporates effects that are essential for the study of orogenic magmatism, such as mineralogical phase changes, fluid release and consumption, partial melting, melt extraction and emplacement. The mechanical equations of momentum (Stokes equation for creeping flow) and mass (continuity equation) are solved for a compressible non-Newtonian, visco-plastic fluid. Solving the energy equation, which accounts for latent, adiabatic, radiogenic and shear heat production, simulates the thermal evolution of the model. A detailed description of the numerical approach is given in Gerya and Yuen (2003a, 2003b), Gerya and Burg (2007) and Gerya (2010).

2.1. Initial configuration

The 2D computational domain covers 4000 km $\times$ 1400 km with a resolution of 1361 $\times$ 351 nodal points (Fig. 1). The numerical resolution increases from 10 $\times$ 10 km to 1 $\times$ 1 km towards the centre of the domain, i.e. area undergoing subduction and collision. All boundaries are free slip. The setup simulates subduction beneath a passive continental margin and includes a gradual change in crustal and sediment composition (Fig. 1a, e.g., Regenauer-Lieb et al., 2001). An imposed constant convergence velocity of 5 cm/yr induces subduction. This velocity condition is deactivated at the onset of collision, i.e. after ocean closure. Subsequent collision is driven by the pull of the subducted slab. The collision and convergence stop in our models after slab detachment.

The oceanic crust is composed of a 2 km thick layer of hydrothermally altered basalt and a 5 km thick layer of gabbro (Tables 1 and 2). The upper plate is composed of a 20 km thick upper and a 20 km thick lower crust (e.g., Kelemen and Behn, 2016) of varying rheology (Fig. 1b; Table 3). The underlying lithospheric mantle is 80 km thick and composed of anhydrous peridotite. The thermal distribution of the oceanic lithosphere is calculated from its thermal cooling age (Table 3, Turcotte and Schubert, 2002). The thermal distribution of the continental lithosphere is calculated following a linear increase from 273 K at the surface to 767 K at the Moho and 1617 K at the lithosphere/asthenosphere boundary. For the asthenospheric mantle, a thermal gradient of 0.5 K/km is used. The setup simulates rapid subduction of a medium to small sized ocean (400–800 km in 8–16 My).

The model assumes instantaneous melt propagation and emplacement after extraction. Processes modifying the primary magma composition, such as fractional crystallization, crustal assimilation and magma mixing are not included. Furthermore, the model assumes partial melting of individual sources (Fig. 1) and does not account for more complex interactions resulting in melting processes such as for instance vein + wall-rock melting (Foley, 1992). However, the variability of the magmatic source and the nature of partial melting and/or melt extraction are resolved to a first order by our numerical approach.

3. Results

We performed a series of numerical experiments (Table 3) to investigate the dynamics and physical controls of magmatism during subduction and subsequent collision. We first describe a reference model that exhibits patterns of magma migration and compositional changes. This is followed by a parametric study, in which we analyse the influence of varies rheologies, thermal slab ages, ocean sizes and convergence rates.

3.1. Reference model

The reference model (sofc, Table 3, Fig. 2) contains a compositionally and rheologically layered continental crust: weak felsic upper crust (wet quartzite) and strong mafic lower crust (plagioclase), which results in low coupling at their interface (Fig. 1b2). In this model, the initial ocean is 400 km wide and has a thermal age of 80 Ma. The lower plate is pushed with 5 cm/year towards the upper plate, which remains fixed. The results show a complex spatial and temporal pattern of compositionally variable magmatic sources activated during oceanic subduction, continental collision and after slab detachment (Figs. 2 and 3).

At the onset of oceanic subduction (<3 My) partial melting of the oceanic crust forms adakites within the upper plate (Fig. 3, sensu Defant and Drummond, 1990; Drummond et al., 1996). After 5 My, the oceanic lithosphere releases volatiles and hydrates the overlying mantle wedge as it sinks deeper into the mantle. The addition of volatiles at depths of ~100 km triggers fluid-fluxed melting of hydrated peridotite in the mantle wedge, which is also associated with melting of the subducted oceanic crust (Figs. 2a and 3, stage 1). These melts penetrate the overriding plate and form flattened plutons at the transition between the lower and upper continental crust and/or by building a volcanic arc at the surface. In our reference model the magmatic arc is observed in the upper plate at ~250 km distance from the trench (position 1 in Fig. 2a). The continuous generation and propagation of melts weakens the overlying continental lithosphere, which results in small amounts of localized extension and subsidence overlaying the thermal anomaly induced by the magmatism (sensu Turcotte and Schubert, 1982). The total magmatic addition rate during this phase equals to 35 km^3/km/My.

The closure of the ocean at 8 My is followed by continental subduction of the lower plate (Fig. 2c), driven by the pull of the slab before slab break-off which ceases subduction at 32 My. Rheological decoupling between the upper and lower continental crust activates a basal decollement at their interface. This decollement facilitates the incorporation of most of the upper crust of the lower plate into the orogenic wedge. The strong coupling between decollement and brittle overburden favours a sequence of foreland propagating thrusts (such thrusts

Table 1
Thermal parameters used in the experiments. k is thermal conductivity (Clauser and Huenges, 1995). H_r is the radioactive heat production and H_L represents latent heat production. $T_{solidus}$ and $T_{liquideus}$, respectively, are solidus and liquidus temperatures of the rocks at given pressure and rock composition. For all rocks: Heat capacity Cp = 1000 J/K; coefficient of thermal expansion $\alpha = 3 \times 10^{-5}$ (1/K), coefficient of thermal compressibility $\beta = 1 \times 10^{-5}$ (1/MPa).

Material; melt generated by melting of that material; magmatic rock crystalized from those melts	k [W/(m∗K)] (at T_K, P_{MPa}) (1)	H_r [μW/m³] (2)	H_L [kJ/kg] (2, 3)	$T_{solidus}$ [K] (at P_{MPa}) (4)	$Tl_{iquidus}$ [K] (at P_{MPa}) (4)
Sediment; melt	$[0.64 + \frac{807}{T+77}] * \exp(4 * 10^{-6} * P)$	2	300	At P < 1200 MPa: $889 + \frac{1.79*10^4}{P+54} + \frac{2.02*10^4}{(P+54)^2}$ At P > 1200 MPa: $831 + 0.06 * P$	$1262 + 0.09 * P$
Upper continental crust; melt	$[0.64 + \frac{807}{T+77}] * \exp(4 * 10^{-6} * P)$	1.8	300	At P < 1200 MPa: $889 + \frac{1.79*10^4}{P+54} + \frac{2.02*10^4}{(P+54)^2}$ At P > 1200 MPa: $831 + 0.06 * P$	$1262 + 0.09 * P$
Lower continental; lower oceanic crust; melt	$[1.18 + \frac{474}{T+77}] * \exp(4 * 10^{-6} * P)$	0.18	380	At P < 1600 MPa: $973 - \frac{7.04*10^4}{P+354} + \frac{7.78*10^7}{(P+354)^2}$ At P > 1600 MPa: $935 + 35 * 10^{-4} * P + 62 * 10^{-7} * P^2$	$1423 + 0.105 * P$
Upper oceanic crust (basalt); melt	$[1.18 + \frac{474}{T+77}] * \exp(4 * 10^{-6} * P)$	0.18	380	At P < 1600 MPa: $973 - \frac{7.04*10^4}{P+354} + \frac{7.78*10^7}{(P+354)^2}$ At P > 1600 MPa: $935 + 35 * 10^{-4} * P + 62 * 10^{-7} * P^2$	$1423 + 0.105 * P$
Lithospheric/asthenospheric dry mantle	$[0.73 + \frac{1293}{T+77}] * \exp(4 * 10^{-6} * P)$	0.022	–	$1394 + 0.133 * P_{MPa} + 51 * 10^{-7} * P^2_{MPa}$	$2073 + 0.114 * P$
Wet mantle; melt (dry and wet mantle)	$[0.73 + \frac{1293}{T+77}] * \exp(1+4 * 10^{-6} * P)$	0.022	300	At P < 1600 MPa: $973 - \frac{7.04*10^4}{P+354} + \frac{7.78*10^7}{(P+354)^2}$ At P > 1600 MPa: $935 + 35 * 10^{-4} * P + 62 * 10^{-7} * P^2$	$2073 + 0.114 * P$
Serpentinized mantle	$[0.73 + \frac{1293}{T+77}] * \exp(1+4 * 10^{-6} * P)$	0.022	–	At P < 1600 MPa: $973 - \frac{7.04*10^4}{P+354} + \frac{7.78*10^7}{(P+354)^2}$ At P > 1600 MPa: $935 + 35 * 10^{-4} * P + 62 * 10^{-7} * P^2$	$2073 + 0.114 * P$
Depleted mantle	$[0.73 + \frac{1293}{T+77}] * \exp(1+4 * 10^{-6} * P)$	0.022	–	At P < 1600 MPa: $973 - \frac{7.04*10^4}{P+354} + \frac{7.78*10^7}{(P+354)^2}$ At P > 1600 MPa: $935 + 35 * 10^{-4} * P + 62 * 10^{-7} * P^2$	$2073 + 0.114 * P$

migrate towards the left in Fig. 2c). The lower crust of the upper plate indents the sutured oceanic subduction zone and promotes the formation of back-thrusts, along which material is transported towards the hinterland. The indentation – and thrust – related topography suppresses wedge widening caused by frontal accretion and prevents the formation of the otherwise common collisional out-of-sequence deformation. The lower crust of the lower plate remains coupled to its mantle lithosphere and, therefore, subducts beneath the upper plate. Slivers of upper crust (thin light-grey stripes in Fig. 2c) are dragged into the subduction channel along with sediments from the accretionary wedge and may reach mantle depths of up to 120 km. These slivers are incorporated into a melange that includes parts of oceanic crust and serpentinized and hydrated mantle.

In the hinterland of the upper plate (right side of Fig. 2c), extension is localized along listric normal faults that are rooted in a basal decollement at the transition between the upper and lower continental crust. The activation of normal faults migrates gradually towards the foreland (to the left in Fig. 2c). Interestingly, the lower crust of the upper plate remains relatively little deformed. The difference in shortening between the upper and lower crust results in lower crustal indentation of the orogenic wedge, composed of the oceanic suture, accretionary wedge and upper crust. Consequently, the orogenic wedge is pushed over a significant distance towards the hinterland (to the right in Fig. 2c–g). This creates a gradual shift between the former suture created during oceanic subduction and the currently active continental subduction zone that increases with time (Fig. 2c, e, g). Because of its positive buoyancy and low viscosity, the melange moves upwards along the subduction channel, and relaminates (sensu Hacker et al., 2011) the base of the crust at the core of the orogen at around 18 My (~40 km depth, Fig. 2c, e, g). At the same time, the lower plate detaches from the mantle lithosphere of the upper plate, which results in slab steepening and asthenospheric upwelling. The asthenospheric upwelling is initially associated with partial melting of wet peridotite, resulting in the creation of small volumes of basaltic melt. These melts are emplaced in the upper plate using normal faults as transport pathways (position 2, Figs. 2c and 3). The large temperature contrast between the subducted crust and hot asthenosphere causes partial melting of the rock melange in the subduction channel and the lower continental crust. The resulting felsic melts are emplaced in the hinterland of the upper plate ~120 km away from the tip of the lower crust indentor (position 3 in Fig. 2e). During this continental subduction stage melting occurs from three compositionally different components: a decreasing proportion of wet peridotite (57% to 25%), an increasing proportion of lower continental crust (8% to 35%) and a slightly increasing proportion of rock melange (cumulative sediments, upper continental crust, oceanic crust, 35% to 40%) sources (positions 3 and 4 and stages 3 and 4 in Figs. 2e, g and 3). During later collisional stages, the back-arc hinterland of the upper plate records shortening, because the frontal crustal accretion is not anymore accommodated entirely by foreland thrusting due to upper crustal thickening. Consequently, large parts of the shortening associated with accretion is transferred to the hinterland. Reverse faults and folds are formed that act as magma transport pathways

Table 2
Ductile creep parameters of different rheologies involved in experiments. Density - ρ_0; pre - exponential factor - A_D; activation energy - E_a; stress exponent – n; activation volume - V_a; cohesion – C; friction angle – sin(φdry). The flow laws are defined in Ranalli (1995) and references therein.

Material	ρ_0 [kg/m³]	Flow law	$1/A_D$ (Pa^n*s)	E_a [kJ/mol]	n	V_a [J/bar/mol]	C [MPa]	sin(φdry)
Sediments	2600	Wet quartzite	$1.97 * 10^{17}$	$1.54 * 10^5$	2.3	0.8	10	0.15
Upper continental crust	2700							0.3
Upper oceanic crust (basalt)	3000							0.2
Melts derived from sediments, upper and lower continental crust	2400	Wet quartzite	$5 * 10^{15}$	0	1	0	10	0
Lower continental crust	2900	Plagioclase (An75)	$4.8 * 10^{22}$	$2.38 * 10^5$	2.3	0.8	10	0.3
Lower oceanic crust (gabbro)	3000	Plagioclase (An75)	$4.8 * 10^{22}$	$2.38 * 10^5$	3.2	0.8	10	0.6
Melt derived from subducted oceanic crust	2900	Wet quartzite	$1 * 10^{13}$	0	1	0	10	0
Lithosphere/asthenospheric dry mantle	3300	Dry olivine	$3.98 * 10^{16}$	$5.32 * 10^5$	3.5	0.8	10	0.6
Depleted mantle	3200							
Hydrated mantle and weak initial shear zone	3200	Wet olivine	$5.01 * 10^{20}$	$4.70 * 10^5$	4	0.8	10	0.1
Serpentinized mantle	3000							
Melt derived from wet peridotite	2900	Wet olivine	$1 * 10^{13}$	0	1	0	10	0

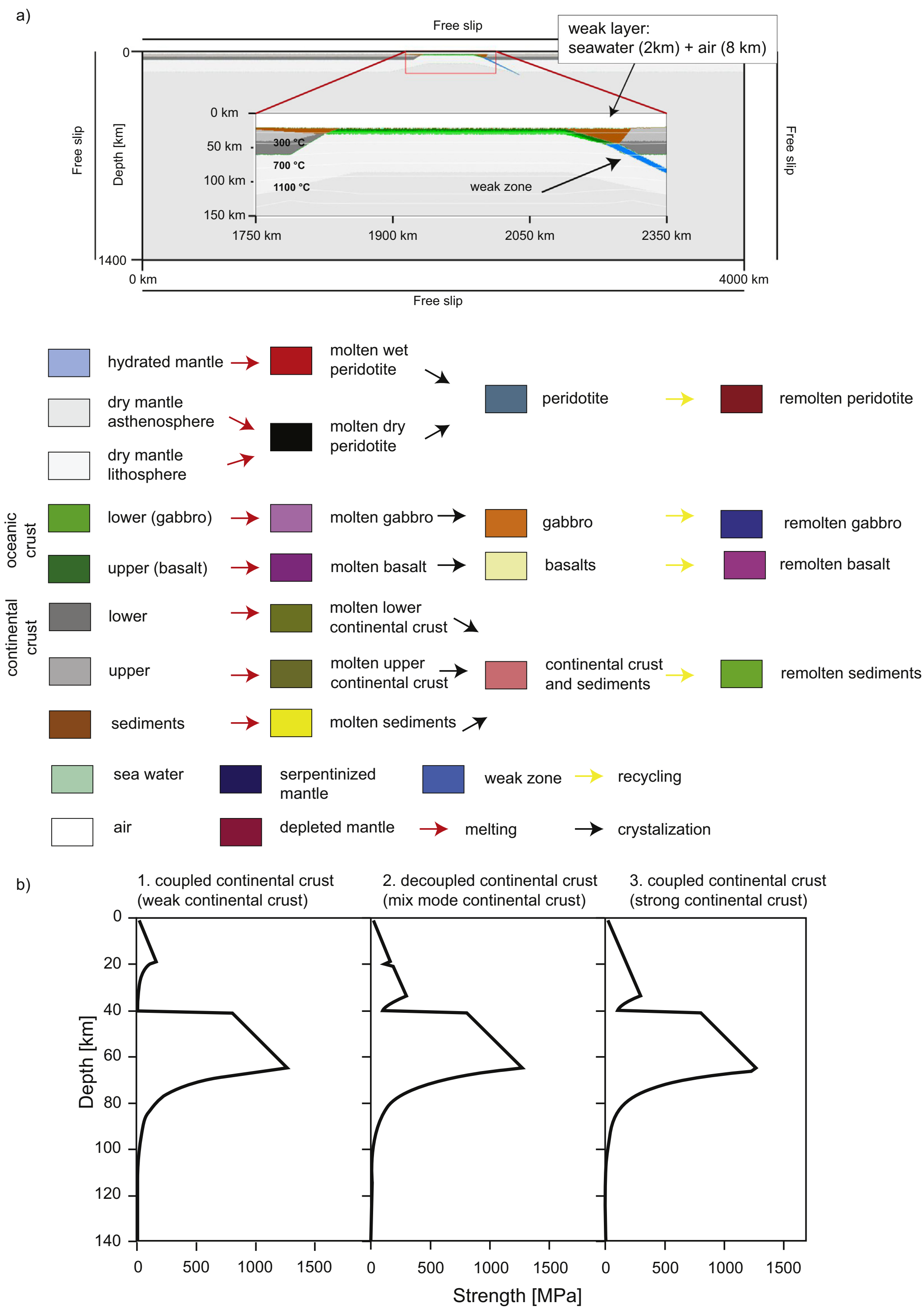

Fig. 1. a) Initial model setup (see text for details). White lines represent isotherms in °C in increments of 200 °C starting from 100 °C. Materials (e.g., rock, melt, air) that appear in the following figures are defined by colors. The mantle is represented by two colors (two layers with same physical properties) to illustrate mantle flow; b) Initial strength profile of the continental lithosphere for a constant strain rate of $\dot{\varepsilon} = 10^{-14}\ s^{-1}$. Three initial strength profiles are used (1) coupled weak continental crust, (2) decoupled mixed mode continental crust and (3) coupled strong continental crust.

(Fig. 2e). The continuation of subduction brings more continental material into the subduction channel, generating melts that are increasingly more felsic (position 4 in Figs. 2g and 3). At this stage, the deformation in the back-arc of the upper plate changes from compression to extension. Normal faults are formed allowing for magma transport and emplacement (Fig. 2g). In the foreland, in sequence thrusting is favoured by moderate steepening of the basal decollement and underthrusting induced by the upward buoyant flow of material along the subduction channel, which prevents the accreting wedge to reach a subcritical state and experience out-of-sequence thrusting.

Table 3
Summary of all performed numerical experiments.

Ocean length	400 km	800 km	400 km	400 km	400 km	400 km	400 km	400 km
Age of oceanic lithosphere/convergence rate	5 cm/yr (lower plate)	5 cm/yr (lower plate)	5 cm/yr (lower plate)	5 cm/yr (lower plate)	5 cm/yr (lower plate) + 3 cm/yr (upper plate)	Symmetric convergence, 2.5 cm/yr	2.5 cm/yr (lower plate)	7.5 cm/yr (lower plate)
20 Ma	sofi							
40 Ma	sofa							
60 Ma	sofb							
80 Ma	sofc	vicc	ijac	spfc	migc	symd	slac	dorc
100 Ma	sofd							
120 Ma	sofe							
Duration of the push	Until collision	Until 400 km of ocean was consumed	Until collision	Until collision	Until 400 km of ocean was consumed	Until collision	Until collision	Until collision
Continental crust	Mix mode*	Mix mode*	Weak*	Strong*	Mix mode*	Mix mode*	Mix mode*	Mix mode*

Mix mode * - upper (wet quartzite) and lower (An75_Ranalli, 1995) crust.
Weak * - upper and lower crust (wet quartzite).
Strong * - upper and lower crust (An75_Ranalli, 1995).

Finally, slab detachment separates the oceanic and continental part of the slab at 33 My. Slab detachment is followed by exhumation of the lower plate by reversing the motion of the subduction plane (i.e. by eduction, sensu lato Andersen et al., 1991, Fig. 2i). Slab detachment combined with exhumation and partial melting of large parts of the lower continental crust induce a decrease in the slab dip. Eduction uplifts the previously relaminated melange and reactivates the former thrusts as low-angle normal faults or detachments. These structures exhume upper crustal material from depths of ~15–20 km and temperatures of T = 500 °C–550 °C (position 5 in Fig. 2i). The exhumation is associated with partial melting of the upper continental crust and emplacement of felsic melts (stage 5 in Fig. 3). Furthermore, low-angle normal faults or detachments are used as magma transport pathways, resulting in the formation of either core-complexes or extensional domes (e.g., Tirel et al., 2004, position 5 in Fig. 2i).

3.2. The influence of rheological stratification of the continental crust

The rheological stratification of the continental lithosphere has a fundamental impact on the kinematics, evolution and geometry of continental collision. Starting from the reference model, two extreme scenarios were performed. First, (Fig. 4a–c) we consider the collision of weak continental plates. The entire crust has a wet quartzite rheology in this experiment (Figs. 1b1, 4a–b and Table 3). Second, we examine the collision of two strong continental plates. In this experiment the entire crust has a plagioclase rheology (Figs. 1b3, 4d–f and Table 3). Although the occurrence of such homogeneous crustal profiles is unlikely in nature, we consider these scenarios suitable for illustrating extreme collisional geometries and associated magmatism. In both cases, parts of the upper oceanic crust and accretionary wedge sediments are incorporated into the subduction channel during oceanic subduction (Fig. 4a, d). Magmatism results in minor amounts of extension in the hinterland of the upper plate by weakening above the rising thermal anomaly during magmatism. Melt production is restricted to flux melting of the hydrated mantle wedge, similar to the reference model. In the weak-rheology scenario these melts form intrusions at the base of the crust and extrusions at the surface. In the strong-rheology scenario intra-crustal intrusions and surface extrusions are formed instead (position 1 in Fig. 4a and d, respectively).

In the weak-rheology scenario, collision is characterized by decoupling of crust and mantle (Fig. 1b1). Only minor amounts of crust and sediment from the accretionary prism are transported into the subduction channel. Thickening of the entire crust accommodates crustal shortening and no continental subduction is recorded (Fig. 4b). Slab detachment at the transition between continental and oceanic lithosphere at depths of ~160 km occurs shortly after the onset of collision (~1.5 My) (Fig. 4b) and is followed by isostatic rebound (Fig. 4c). Melting of wet peridotite, subducted melange and crust of the lower plate creates dominantly felsic magmas that are emplaced as intrusions and extrusions in the core of the thickened orogen and in its frontal parts (positions 2 and 3, Fig. 4b). The continued orogenic thickening is associated with a gradual increase in temperatures at the base of the crust, triggering additional melting at the base of the crust (position 4, Fig. 4c).

In contrast, collision of two strong continental plates results in large amounts of continental subduction due to the large degree of rheological coupling. This creates large volumes of crust-derived melts that are emplaced roughly in the same position when compared with magmas formed during oceanic subduction (Fig. 4e, f). Subsequent continental subduction continues until slab detachment ceases convergence at ~32 My. The slab detaches at the transition between continental and oceanic lithosphere at depths of ~300 km (Fig. 4f).

3.3. The influence of the ocean size and thermotectonic age, and the convergence velocity

We have performed an additional experiment in which the width of the ocean was enlarged (800 km). All other parameters were kept the same when compared to the reference model (Fig. 5 and Table 3). Deformation geometries, magmatic sources and migration patterns of the magmatic source region are comparable to the reference model (Fig. 5). However, a wider ocean increases the slab-pull force and drags the subducted continental lithosphere to larger depths. Consequently, slab detachment occurs earlier at ~22 My and at greater depth (~450 km) when compared with the reference model (Fig. 5c). Similar to the reference model, slab detachment enables large partial melting of the lower continental plate, exhumes partially molten rock melanges and reactivates former thrusts as low-angle normal faults or detachments. One of the important factors observed to control the kinematics of subduction is the thermal age of the subducting oceanic lithosphere. Starting from the reference model (i.e. thermal age of 80 Ma), we have tested three other scenarios: two with younger (20 and 40 Ma) and one with an older (120 Ma) oceanic plate age (Fig. 6a, b, c). In the first scenario no continental subduction is recorded and no deformation is observed after the closure of the ocean ("arrested" orogen, sensu Ueda et al., 2012). Subduction terminates because of the insignificant slab pull. Melting of wet peridotite and partial melting of the subducting slab forms magmas in the hinterland of the upper plate ~220 km away from the trench. Subduction of slightly older slabs (40 Ma Fig. 6b), on the other hand, enables continental subduction, generating melts in a position closer to the trench (position 2 in Fig. 6b).

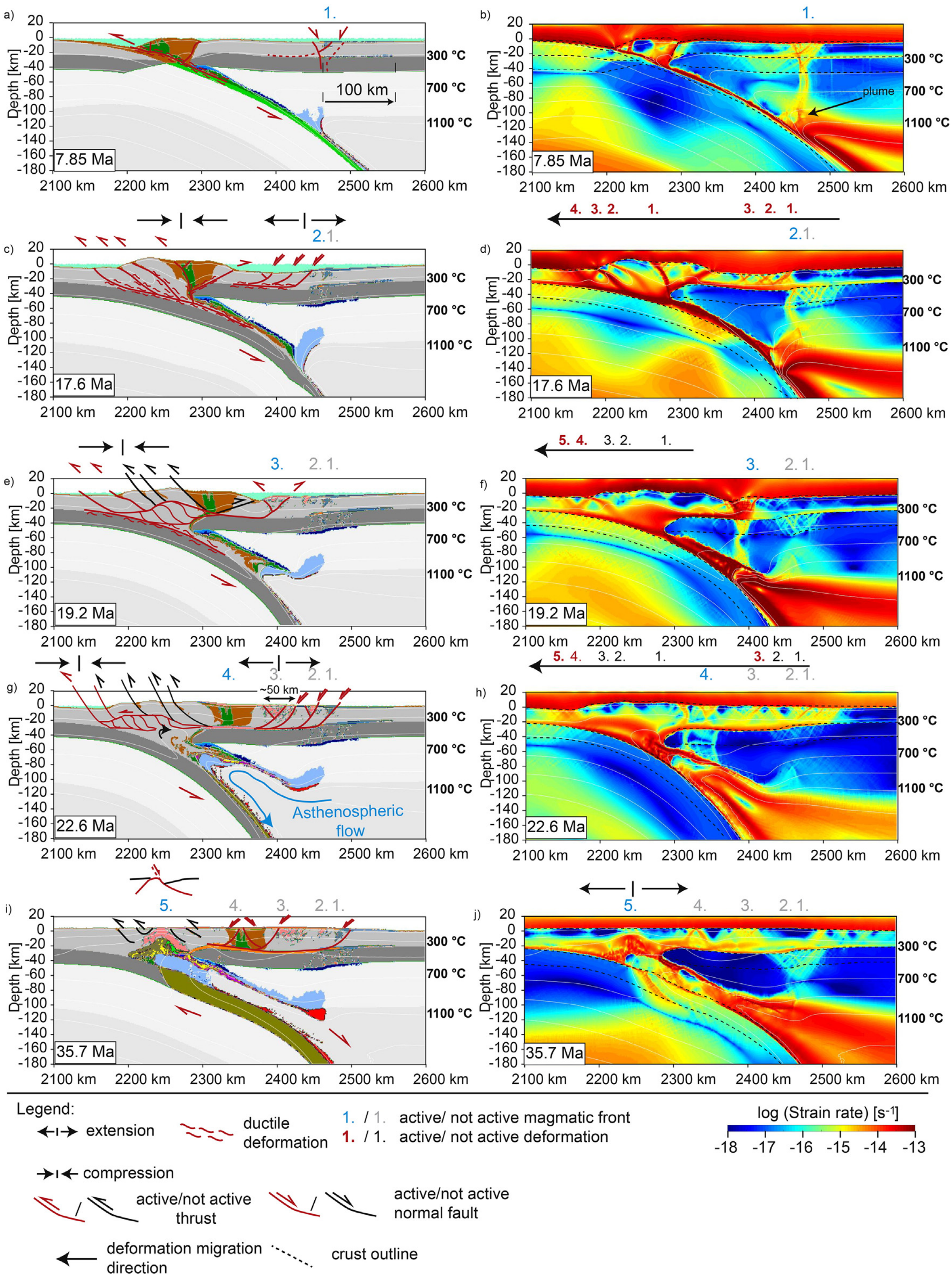

Fig. 2. Evolution of the reference model (sofc, Table 2). The left and right column represent composition and strain rate, respectively. a, b) the first magmatic stage forms by partial melting of wet peridotite during oceanic subduction; c) the second magmatic stage forms during continental subduction and is located 20 km trenchward from the first magmatic arc; d) contemporaneous shortening in the foreland and extension in the hinterland; e, f) the third magmatic stage is syncontractional and forms by partial melting in subduction channel; g) the fourth magmatic stage represents the most felsic magma end-member during continental collision, associated with extension in the hinterland during relamination; h) foreland propagating deformation front; i) the fifth magmatic stage during overall extension driven by eduction; j) eduction triggers exhumation of mid-crustal rocks to the surface along low-angle detachments. Thick black arrows highlight the sense of shear on the subduction plane. See Fig. 1 for color (material) description.

Subduction of older lithosphere (120 Ma Fig. 6c) results in similar collisional and magmatic patterns when compared to the reference model. It also records indentation of the orogenic wedge by the lower crust of the upper plate as described for the reference model. Indentation of the orogenic wedge results in subduction zone and magma source migration. However, much larger amounts of melt are released

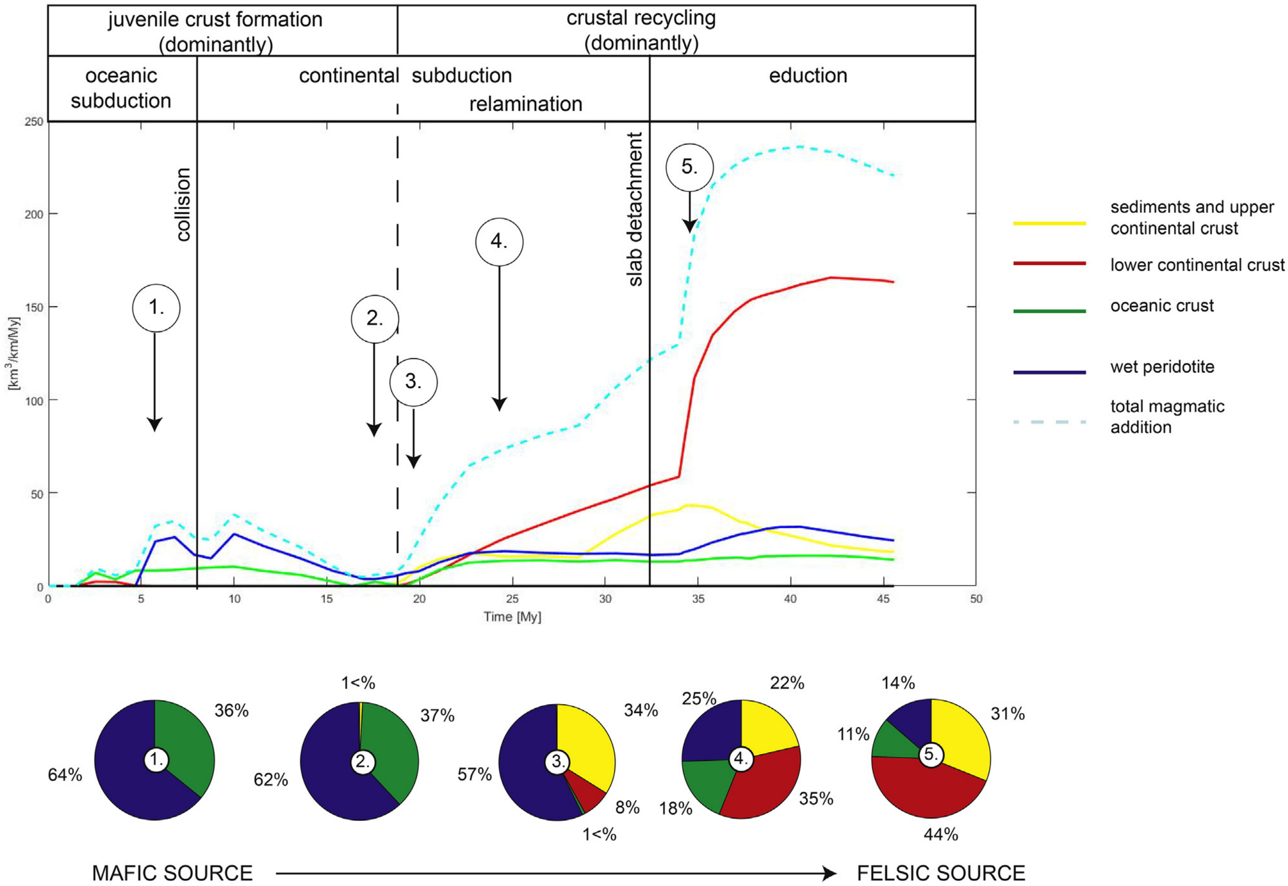

Fig. 3. Source variability and magmatic addition rates for the reference model. Note that 1 to 5 represent the magmatic stages described in Fig. 2, from oldest to youngest.

when compared to the reference model, particularly during the late collisional stage. These melts are emplaced dominantly in the upper plate, at the base of the upper crust (Fig. 6c).

The effects of the convergence velocity were tested in two models. In a first model the upper and lower plate converge with 3 cm/yr and 5 cm/yr, respectively. This model shows a shallow dipping subduction zone during oceanic subduction and no significant lower crustal indentation. During continental subduction, the model is characterized by a low degree of coupling between the lower and upper plate, which ultimately leads to more pronounced slab steepening, larger asthenospheric uprise and the formation of larger volumes of melt when compared to the reference model. These melts are emplaced in the upper plate and the magmatic front gradually migrates towards the foreland with time (Fig. 6d). The final geometry is similar to the one obtained by subduction of a wider ocean (compare with Fig. 5c). The second model assumes symmetric convergence velocities of 2.5 cm/y (Fig. 6e). The model shows indentation of the orogenic wedge by the lower crust of the upper plate during collision. Consequently, significant amounts of shortening are recorded in the upper plate and a gradually increasing shift between the slab and the position of the former oceanic suture zone is observed. The observed magmatism is related to flux melting during oceanic subduction and relamination during continental subduction.

4. Discussion

Our results show that continental subduction in the chosen Mediterranean collisional setting is driven by the pull exerted by the oceanic slab that remains attached to the continental lithosphere. This is related to the strong rheological coupling of lower crust and mantle lithosphere, as suggested by previous studies (e.g., Burov and Yamato, 2008). In contrast, rheological decoupling between crust and mantle lithosphere leads to crustal accretion, similar to ocean-continent subduction settings (e.g., Faccenda et al., 2009; Vogt et al., 2017a, 2017b). In our models, the degree of coupling decreases with an increase of the convergence rate (Fig. 6d, e), or with the increase in slab length (Fig. 5), in agreement with previous inferences (Faccenda et al., 2009). Furthermore, a similar decrease in coupling takes place with an increase of the age of the oceanic lithosphere (Figs. 2, 6a, b), while a fully strong and weak rheology of the entire continental crust has an opposite effect (Fig. 4).

Our reference model shows that a compositionally layered lithosphere creates a mixed collisional mode, in which the upper crust is accreted to form a collisional orogen, while the lower crust is subducted. The resulting orogen is characterized by a sequence of outward propagating thrusts in the orogenic foreland and low-offset extensional (listric) normal faults in the hinterland of the upper plate. The localization of extension is driven by magma emplacement in multiple episodes (see also Gerya and Meilick, 2011). The depth to which the lower crust is subducted depends on the thermal age of the oceanic lithosphere and on the convergence velocity (see also Duretz et al., 2011). The older the slab or the higher its subduction velocity, the greater is the depth of subduction. Deep subduction of the lower crust leads to slab steepening and slab retreat.

Indentation of the orogenic wedge by the lower crust of the upper plate (sensu Oxburgh, 1972) transports crustal material towards the hinterland (Fig. 2c, e, g, i) and creates an increasing shift between the position of the suture zone and the slab, together with its associated

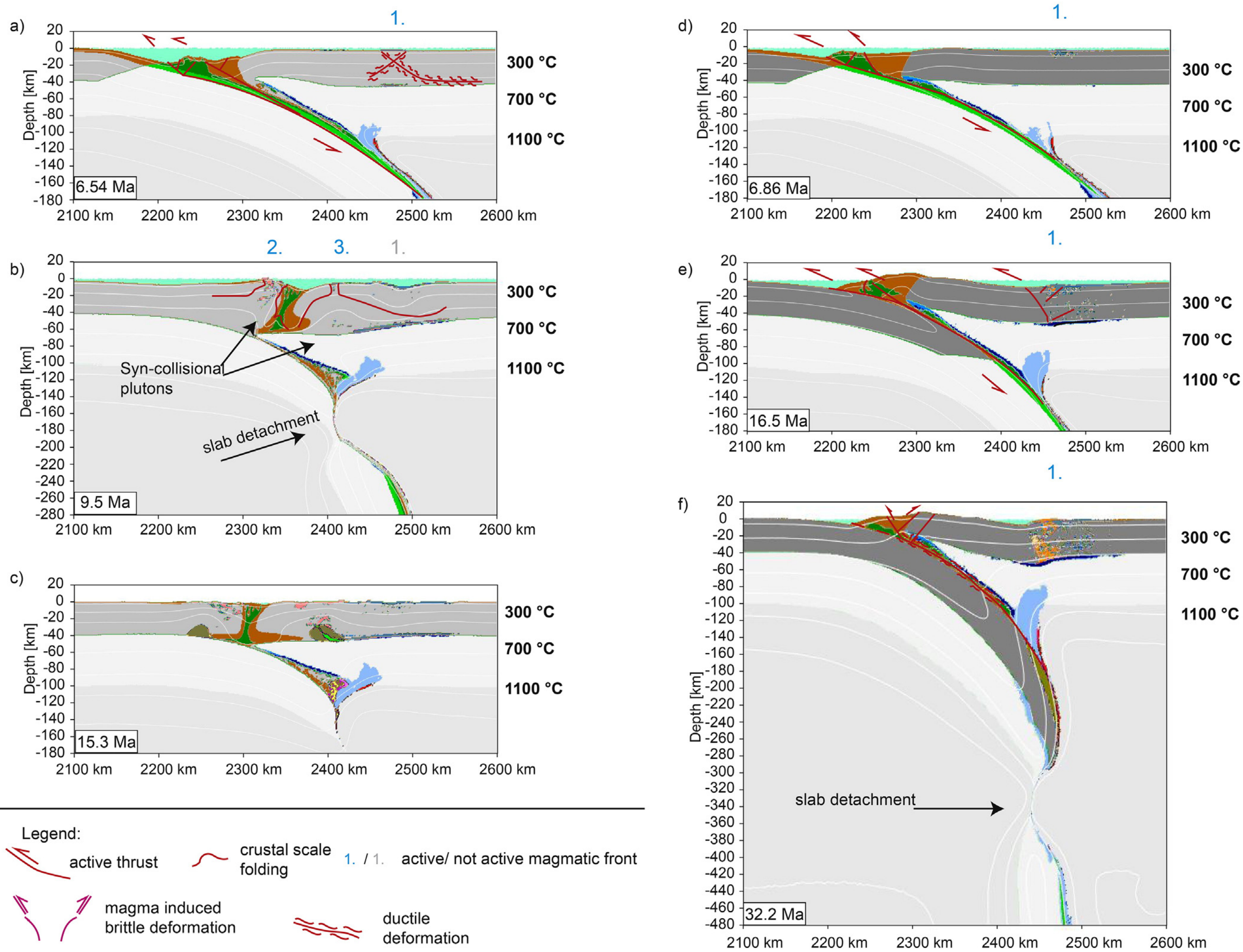

Fig. 4. Evolution of the rheologically weakest (ijac, a–c) and strongest (spfc, d–f) end-member. a) formation of the first magmatic arc during oceanic subduction; b) intrusion of melts derived from partial melting of the subducted melange during crustal scale folding; c) isostatic rebound after slab detachment followed by partial melting of the lower crust; d) flux melting during oceanic subduction forms a magmatic arc; e) during continental subduction the magmatic front remains fixed; f) partial melting of the subducted slab following slab detachment. See Fig. 1 for color (material) description.

deformation and magmatism. Such an indentation process may be applicable in other orogenic systems, for instance during the indentation of the Brazilian Shield into the Andes (e.g., Lamb et al., 1997). In most of our experiments, magma migrates towards the foreland with respect to the former suture zone. The link between magma migration and slab retreat relative to the position of the suture zone has been inferred for many Mediterranean orogens such as the Aegean, Apennines or Dinarides (e.g., Schefer et al., 2011; Menant et al., 2016a). Only in situations where very young oceanic lithosphere is subducted, or where collision of unusually strong and coupled continental lithosphere takes place a fixed magmatic arc is observed, such as possibly in the Pyrennees during the Cretaceous (Figs. 6a and 4d–f, Vissers and Meijer, 2012). The collision of weak continental lithospheres results in a shallow slab detachment and emplacement of magmatic rocks on both sides of the suture (Fig. 4a, b, c). Although such an extreme homogeneous crustal rheology has no obvious natural equivalent, we may speculate that the resulting evolution may be compatible with the Late Eocene–Oligocene magmatism observed along the Peri-Adriatic lineament of the European Alps (e.g., Davies and von Blanckenburg, 1995; Mancktelow et al., 2001). Furthermore, the observed thickening and asymmetry of the crust and upper mantle (Fig. 4b) bear resemblance to previous models accounting for a similarly weak, homogeneous continental crust in collisional settings (e.g., Pysklywec et al., 2002; Pysklywec et al., 2010; Gray and Pysklywec, 2010). In the absence of an inherited oceanic subduction, these models predicted underthrusting/subduction of the upper rigid part of the mantle lithosphere and, in contrast to our experiments, pure shear thickening and subsequent removal of the lower mantle.

The overall magmatic evolution suggested by our models is in agreement with existing numerical modelling and observational studies (e.g., Defant and Drummond, 1990; Vogt et al., 2012). In more detail, migration of magmatism and deformation towards the orogenic foreland is driven initially by the indentation of the lower continental crust in models with a compositionally layered continental lithosphere. The evolution of the slab prior to detachment is driven by a combination of lower crust indentation and the upward buoyant flow of asthenospheric material in the subduction channel (Fig. 2g, i). The migration of magmatism is accompanied by compositional changes that are controlled by melting of different sources, which vary from simple mafic (wet peridotite and oceanic crust) during oceanic subduction, to complex combinations (wet peridotite, oceanic crust, subducted mélange and lower continental crust) during continental subduction and, ultimately, to a dominantly felsic source (upper crustal material) during

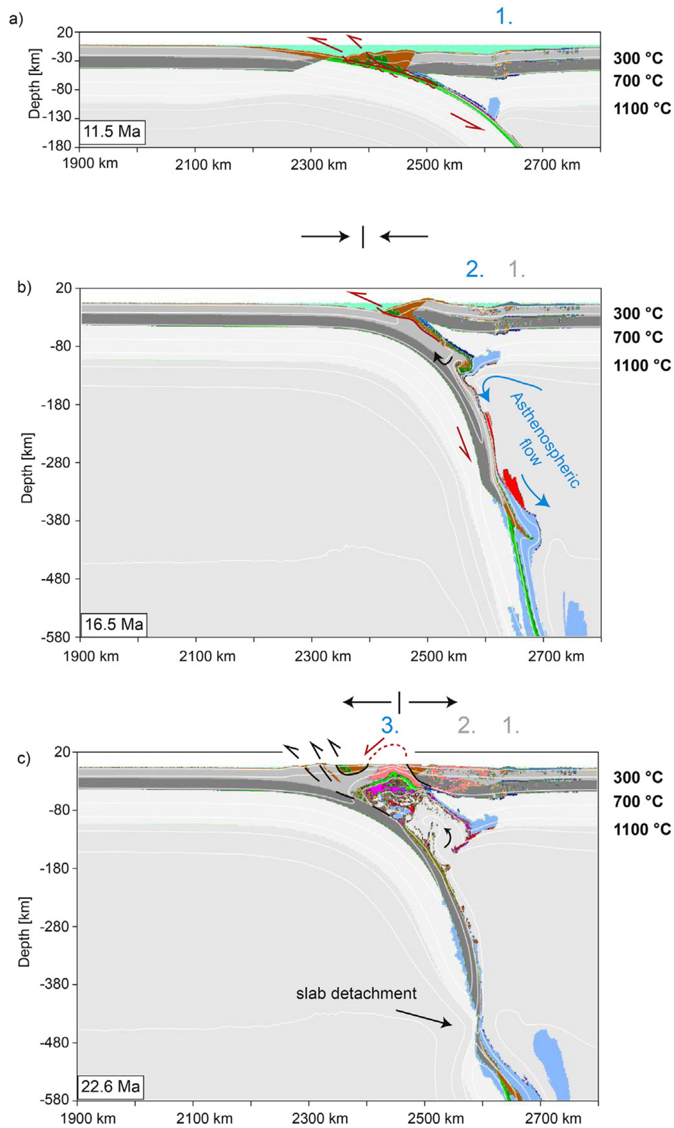

Fig. 5. Evolution in the 800 km wide ocean setting. a) Partial melting of wet peridotite forms the first magmatic arc during oceanic subduction; b) partial melting of the subducted melange forms second magmatic arc; c) reactivation of former thrusts as asymmetric low-angle detachments and exhumation of syn-kinematic magmatic bodies. See Fig. 1 for color (material) description.

eduction (Fig. 3). In contrast, the formation of large amounts of adakite-like magmas (20–40 My, Fig. 6a, b) occurs only where young slabs are consumed in our models. Although subduction of older slabs may also result in the production of adakite-like magmas, their extent and volume is significantly lower in comparison to their younger counterparts (e.g. Figs. 2a and 3). Possible natural equivalents may be located in young and hot slabs along the circum-Pacific margin (e.g. Costa Rica, Aleutian Islands, e.g., Defant et al., 1992; Martin, 1999; Peacock et al., 2005).

4.1. Variability of the magmatic source during continental subduction and exhumation

Magma production is dominated by partial melting of wet peridotite at early stages of subduction and remains active during later stages of collision, but with gradually decreasing contributions in the overall magmatic budget (Fig. 3). Subduction of continental crust involves its partial melting and separation of melts into a mafic residue and a felsic fraction (e.g., Jull and Kelemen, 2001; Kelemen et al., 2003). Driven by its intrinsic buoyancy, this felsic fraction may relaminate to the base of the crust (Hacker et al., 2011). In our models, partial melting of the subducted melange and lower continental crust becomes progressively more important once relamination is triggered. Relamination is driven by the interaction between the asthenospheric mantle and the melange in the subduction channel. The buoyant upraise of material from the subducted melange along the subduction channel stops at the base of the orogen at ~40 km depth. This allows for the emplacement of dominantly felsic magma over a large area (Fig. 2g and i).

Mixtures of wet peridotite, sediment, and other crustal rocks have been generally suggested to explain the source variability of post-collisional (ultrapotassic to calc-alkaline) magmatism in the Mediterranean domain, mostly based on geochemical and isotopic signatures (e.g., Conticelli, 1998; Prelević and Foley, 2007; Conticelli et al., 2011; Prelević et al., 2013). In addition, field and geochemical studies of collisional granitoids in many orogens suggest that these rocks are derived from metaluminious magmas originated from partial melting of mafic lower continental crust (e.g., Christofides et al., 2007).

After slab detachment, the sense of shear along inherited thrust contacts is reversed triggering extension by the formation of major low-angle normal faults or detachments reactivating the former subduction zone or other pre-existing nappe contacts. Footwall exhumation along these structures brings felsic magma from mid-crustal levels to higher structural positions. Coeval adiabatic melting of dominantly crustal material produces peraluminious felsic magmas that are emplaced as syn-kinematic granites or extensional gneiss domes, such as inferred for the Aegean domain during the migration of subduction and back-arc extension (e.g., Tirel et al., 2004; Brun and Faccenna, 2008; Dilek and Altunkaynak, 2009). In our models, slab detachment and shear reversal of the subduction plane are not directly responsible for exhumation of the rocks along the subduction channel (see also Duretz et al., 2012; Duretz and Gerya, 2013). Here the exhumation of rocks starts earlier by the buoyant rise of material towards the surface in the subduction channel (see also Burov et al., 2001). In other words, we observe a two-stage uplift of material from the subduction channel. At first, relamination uplifts the subducted melange from depths of ~120 km to the base of the orogen (40 km). Subsequent shear reversal transports this material from the base of the orogen to mid-crustal levels. This process has been also suggested for the exhumation of UHP-HP terranes, such as in the Western Gneiss Region of Norway (e.g., Liou et al., 1996; Ota et al., 2000).

4.2. The Dinarides Mountains: an example of migration of magmatism in orogens

One of the Mediterranean orogens associated with migration of crustal accretion and magmatism with time towards the orogenic foreland that is well comparable to our modelling is the Dinarides Mountains of Central Europe (Fig. 7a). These mountains formed during the late Mesozoic-earliest Cenozoic closure of the Neotethys Ocean and subsequent continental collision between Europe and Adria (e.g., Dimitrijević, 1997; Karamata, 2006; Schmid et al., 2008). This evolution was followed by the Miocene extension of the Pannonian Basin and its subsequent latest Miocene–Quaternary inversion (Horváth and Cloetingh, 1996), which modified the initial thrusting geometry of the Dinarides units (e.g., Matenco and Radivojević, 2012; Balázs et al., 2016). The tectonic evolution of the Dinarides was associated with significant magmatism that occurred in several successive stages during late Cretaceous-Miocene times (Cvetković et al., 2013). These stages are generally organized in lineaments roughly parallel with the strike of the orogen and show an overall trend of increasing crustal input towards the orogenic foreland (e.g., von Quadt et al., 2003; Cvetković et al., 2013; Gallhofer

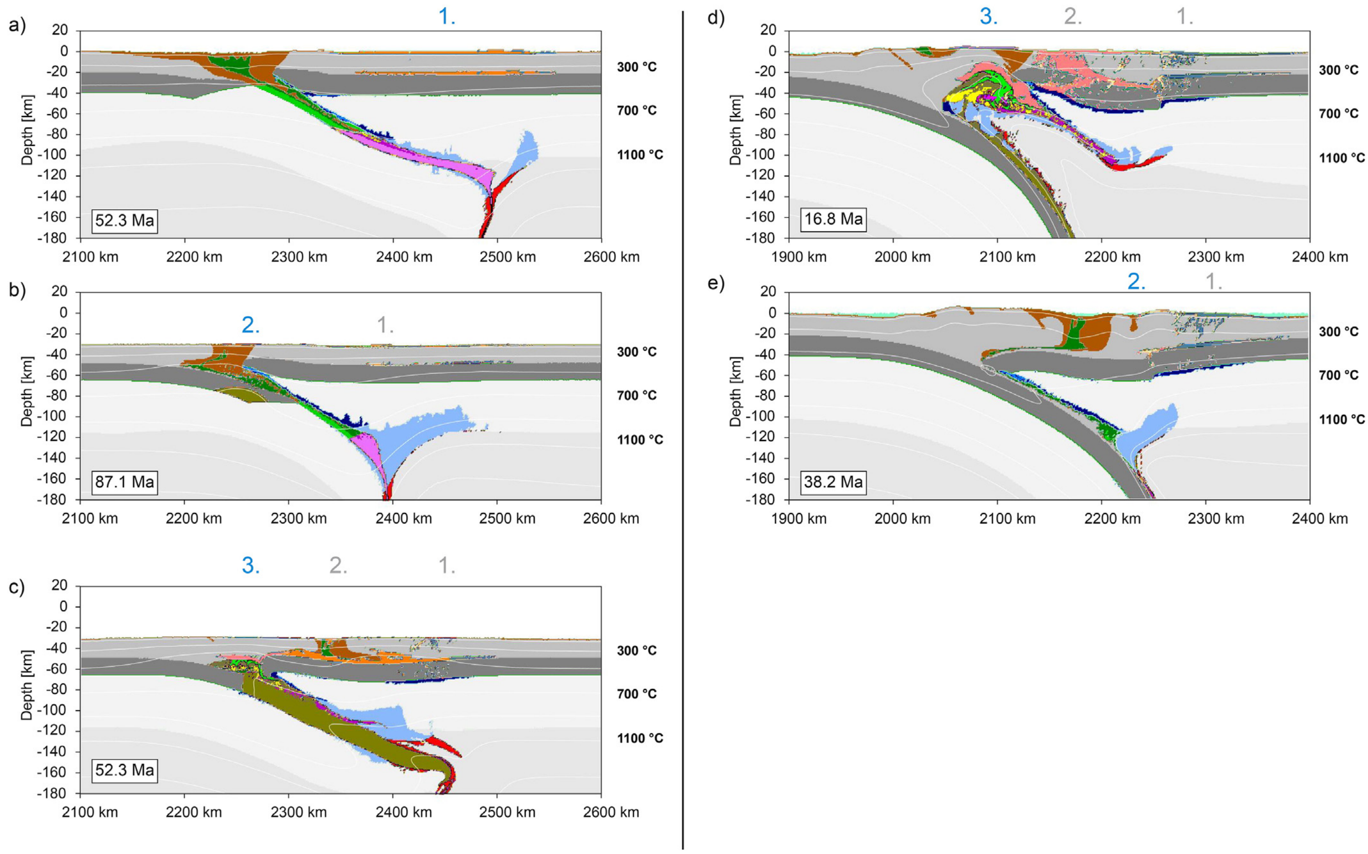

Fig. 6. Variations in lithospheric cooling age (a–c) and convergence rate (d–f); a) Partial melting of hot and young oceanic lithosphere forms a magmatic arc (20 Ma, sofi); b) second magmatic stage caused by partial melting of the lower crust (40 Ma, sofa); c) three stage magmatic evolution without exhumation of syn-kinematic magmatic bodies for old slabs (120 Ma, sofe); d) step-wise migration of the magmatic arc towards the lower plate (migc, asymmetric convergence, 8 cm/yr (lower plate), 3 cm/yr (upper plate); e) syn-contractional magmatism formed during second magmatic phase (symd, symmetric convergence, 2,5 cm/yr). See Fig. 1 for color (material) description.

et al., 2015; Šoštarić et al., 2012). These general observations bear strong similarities with the inferences of our study.

In more detail, oceanic subduction created the first stage of Late Cretaceous (~92–67 Ma) magmatism that is observed in the Apuseni-Banat-Timok-Srednogorie (ABTS) belt, located in the hinterland of the Dinarides orogen (e.g., von Quadt and Peytcheva, 2005; Gallhofer et al., 2015). This stage produced typical arc-related calc-alkaline rocks with a subordinate adakite-like geochemical signature formed by partial melting of subduction-modified wet peridotite in the mantle wedge (e.g., von Quadt et al., 2002; Kolb et al., 2013, Fig. 7b). Kolb et al. (2013) recognized that some of these rocks exhibit adakitic geochemical signatures and inferred the same source as the arc magmas (i.e. wet mantle) via distinct differentiation paths that involved extensive high-pressure amphibole crystallization at lower-crustal conditions. A general foreland age progression is inferred across ~100 km, which is interpreted as the result of either oblique subduction or slab retreat (e.g., von Quadt and Peytcheva, 2005; Kolb et al., 2013; Gallhofer et al., 2015). Field studies have demonstrated a genetic link between magmatic emplacement and the formation of local extensional/transtensional basins/structures, where extrusive and intrusive magmas were emplaced or re-deposited. This is particularly clear in the Timok and Srednogorie sectors of the ABTS belt (e.g., Georgiev et al., 2009; Naydenov et al., 2013). There are no quantitative studies on the amounts of Late Cretaceous extension in these Timok-Srednogorie sectors, but the overall stretching appears to be minor at the orogenic scale. The character of this magmatism and its kinematic relationships are comparable with the initial formation of a stable magmatic arc in our models, where such an arc forms by melting of wet peridotite. However, our model suggests that the adakitic affinity may have been related to melting of oceanic crust during early stages of oceanic subduction (Fig. 2a), in contrast to high-pressure fractionation scenarios (Kolb et al., 2013). The weakening effect of magma transport and emplacement favoured the development of extensional structures in the overriding plate by rheological weakening and rising thermal anomalies (Fig. 8a). Subsequent magmas are emplaced beneath or in the overlying (half-) grabens. Therefore, our model infers that slab-retreat is not required to create the observed Late Cretaceous extension and magma migration patterns in the Dinarides. Furthermore, generic back-arc extension driven by slab retreat was shown to affect the hinterland of magmatic arcs, not the magmatic arc itself (e.g., Uyeda and Kanamori, 1979; Dewey, 1980). In other words, all these observations and modelling results suggest that although slab retreat could have

Fig. 7. a) Tectonic map of the Alpine-Carpathian-Dinaridic system (simplified after Schmid et al., 2008). Black thick line (A–B) represents the location of the profile;in Fig. 7b and the reconstruction of Fig. 8; b) Crustal scale cross-section over the Dinarides (constructed by using the principles described in Schmid et al., 2008) juxtaposed over a regional teleseismic mantle tomography section (Piromallo and Morelli, 2003; Bennett et al., 2008). Location of the section is displayed in Fig. 7a, dotted black line; c) Total alkali vs silica diagram for chemical classification of magmatic rocks (Late Cretaceous to Miocene) in the Dinarides; d) Nd-Sr isotope diagram for same magmatic rocks in the Dinarides (Jovanović et al., 2001; Cvetković et al., 2004a; Prelević et al., 2005; Cvetković et al., 2007b; Zelić et al., 2010; Christofides et al., 2011; Koroneos et al., 2011; Cvetković et al., 2013; Kolb et al., 2013).

taken place during Late Cretaceous times, it is not intrinsically required by the observed relationship between magmatism and tectonics in the hinterland of the Dinarides.

The final closure of the Neotethys Ocean likely took place during latest Cretaceous-earliest Paleogene times by the creation of an oceanic suture zone (~65 Ma, Sava Zone, e.g., Pamić, 2002; Schmid et al., 2008;

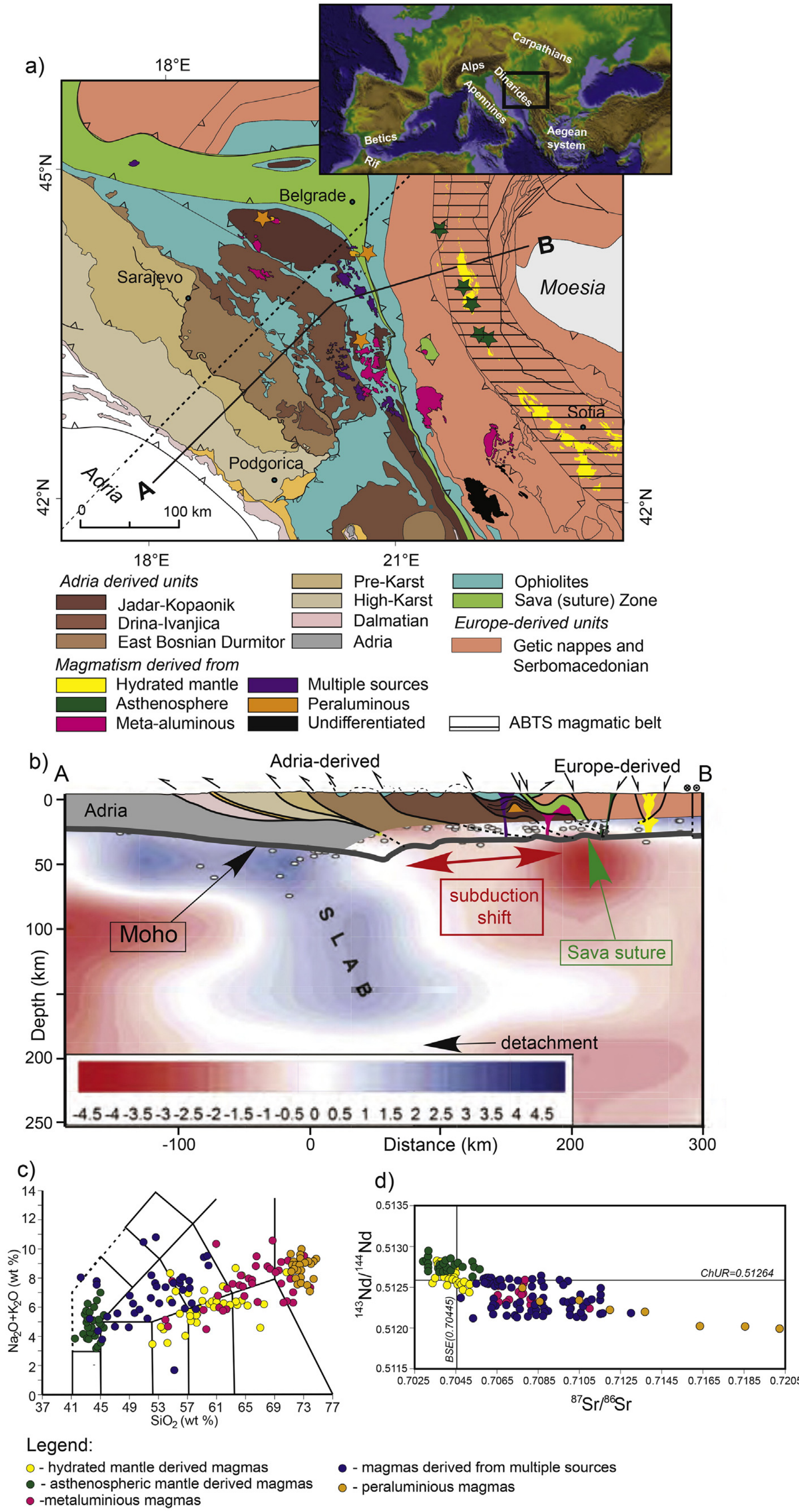

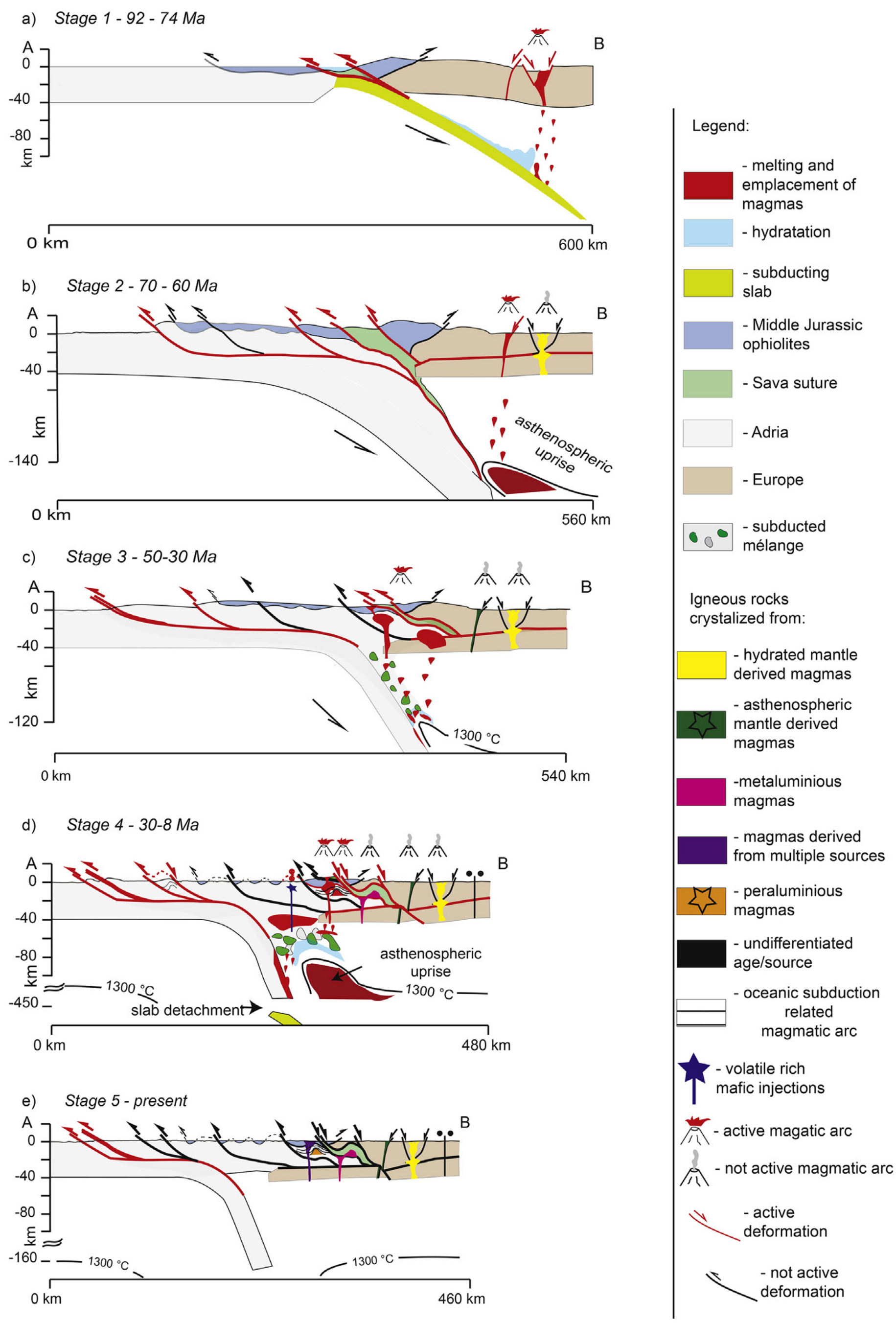

Fig. 8. Interpretative tectono-magmatic reconstruction of the Dinarides. a) production of calc-alkaline magmas in typical continental arc setting during oceanic subduction in the Late Cretaceous; b) monogenic alkaline magmas resulted from partial melting of a metasomatised lithospheric mantle during continental subduction in the (latest Cretaceous?)-Paleogene; c) magma production is driven by partial melting of multiple sources (wet peridotite, subducted melange and lower continental crust) in the subduction channel during relamination in the Eocene–Oligocene; d) generation of magmas produced by multiple sources due to relamination during continental subduction, and subsequent formation of syn-kinematic peraluminious magmas triggered by eduction during the Miocene; e) present day profile. Note that patterns of magmatic bodies reflect different magma sources and not the petrology of crystallized rocks.

Ustaszewski et al., 2010). The convergence continued during Paleogene times, although its kinematic effects and amplitude of deformation in the internal Dinarides are not fully understood (e.g., Matenco and Radivojević, 2012; Stojadinović et al., 2017). At first, the deformation was coeval with the emplacement of a second stage of short-lived latest Cretaceous–earliest Palaeocene (~70–65 Ma) monogenetic mafic alkaline volcanic and subvolcanic bodies. These bodies were emplaced over or intruded into the upper plate mostly along pre-existing fractures formed during localized extension (Fig. 7a, c, d, e.g., Tschegg et al., 2010; Cvetković et al., 2013). Xenoliths found in these magmatic rocks suggest lithospheric temperatures of ~1000 °C (e.g., Cvetković et al., 2004b, 2007a). This magmatism was shown to have formed by partial melting of hydrous mantle (Cvetković et al., 2010). Although, similar to the source of the European Cenozoic anorogenic provinces (e.g., Lustrino and Wilson, 2007; Cvetković et al., 2007a), these small volumes of melts rather reflect a secondary direct sourcing of melts by asthenosphere in the hinterland of the subduction zones, as observed for instance elsewhere in the Mediterranean system (Seghedi and Downes, 2011; Faccenna et al., 2014). These observations are in general agreement with our modelling predictions, where melting of wet peridotite in the mantle wedge at temperatures of >1000 °C continued to produce small volumes of magma (Fig. 8b).

Continued shortening during Eocene-Oligocene times is interpreted as a foreland propagation of thrusting and out-of-sequence reactivations in the external and internal Dinarides, respectively (e.g., Ustaszewski et al., 2010; Andrić et al., 2017; Stojadinović et al., 2017). A gradual switch from contraction to extension took place during Oligocene times in areas situated in the vicinity of the Sava suture zone (Erak et al., 2017; Stojadinović et al., 2017). In the same area, the character of deformation is mirrored by the magmatic evolution that recorded a third stage of coeval magmatic emplacement located more to the foreland when compared with the earlier Late Cretaceous-Palaeocene magmatism (Fig. 7a, c). This Eocene-Oligocene magmatism was emplaced as dominantly medium- to high- potassic calc-alkaline plutons and their extrusive equivalents derived from I-type metaluminious granitoid magmas (e.g., Cvetković et al., 2007b). The elevated contents of large ion lithophille elements, low Sr-Nd isotope ratios together with rare earth element patterns suggest a source located in the uppermost mantle or lower crust (e.g., Cvetković et al., 2007b; Schefer et al., 2011). The larger volumes of predominantly acid to intermediate rocks are associated with lower amounts of volcanic and sub-volcanic potassic to ultra-potassic rocks with mafic to even ultramafic compositions. They are thought to be derived from a source composed of depleted peridotite and terrigenous trench sediments accreted beneath the lithosphere of the upper plate (Prelević et al., 2005, 2013), possibly related to slab roll-back (Schefer et al., 2011). These observations are in agreement with our reference model, which predicts the migration of deformation and magmatism towards the foreland with respect to the suture zone before the onset of slab detachment. Here magmatism is triggered by relamination of crustal material to the base of the orogen and partial melting of wet peridotite, subducted melange and lower continental crust in the subduction channel (Fig. 2d–g).

The Miocene extension reactivated inherited nappe contacts, which led to exhumation of material from mid-crustal levels in the footwall of detachments or low-angle normal faults. This is well observed in large areas in the Dinarides, with larger offsets in their internal part and neighbouring southern Pannonian Basin, along the pre-existing Sava suture zone (e.g., Ustaszewski et al., 2010; Stojadinović et al., 2013), but also along the nappe contacts in more external units, such as observed in the Sarajevo Basin (Fig. 7a, Andrić et al., 2017). The exhumation induced isothermal decompressional melting and the formation of peraluminous magmas (Fig. 8d, e.g., Cvetković et al., 2007a; Schefer et al., 2011). Small volumes of magmatic bodies occurring only in the internal Dinarides characterize this Miocene extension-related magmatic stage. Our modelling demonstrates that the widespread Miocene extension was associated with the emplacement of dominantly felsic melts from the upper crust (Figs. 2i and 8d) and the rheological weakening created during previous magmatic stages. All these observations correlated with modelling infer that the Miocene extension was related to a kinematic reversal along the subduction plane, or in other words with eduction.

The kinematic and magmatic observations in the Dinarides show that in the Oligocene deformation changed gradually from contraction to extension over ~8 My. Our modelling shows that this gradual change could be controlled by progressive slab detachment, resulting in a change from Eocene relamination and contraction to Miocene eduction and extension. The extension observed near the Sava Zone (sensu Matenco and Radivojević, 2012) has started ~28–29 Ma (Toljić et al., 2013; Erak et al., 2017; Stojadinović et al., 2017). When combined with the predictions of our modelling, this imposes that the overall Oligocene-Miocene orogenic extension took place during and after the slab-detachment in the Dinarides.

The Miocene extension was followed by the latest Miocene-Quaternary indentation of Adria driven by the larger scale convergence between European and African plates. This large-scale process created a wide zone of interaction between thrusting and/or lower crustal indentation in the Alps, Apennines and Dinarides (e.g., Handy et al., 2010). In the Dinarides, this indentation inverted the extensional basins and created large scale thrusting that was recorded with larger effects in the internal units in the NW and in the external units in the SE, leading to the large scale thrusting and seismicity (e.g., Herak et al., 1995; Tomljenović and Csontos, 2001; Bennett et al., 2008; Kastelic and Carafa, 2012). Seismicity, teleseismic tomography, potential field data and active seismic experiments show that this recently active deformation is associated with a slab fragment presently located beneath the external Dinarides (Fig. 7b, e.g., Bennett et al., 2008; Šumanovac and Dudjak, 2016). Our model cannot explain the post-Miocene thrusting because it does not take into account the large-scale interaction during the Adriatic indentation. However, our model can largely explain the presently observed foreland shift of 100 km between the position of the Sava suture zone and the present-day location of the Dinarides slab, which is compatible with our model geometry (Fig. 2i). Such shifts and plate configurations are also common in other collisional orogens in the Mediterranean domain (Apennines, Betics-Rif, Carpathians) that show retreating subduction boundaries, steep slabs, back-arc extension and migration of magmatic fronts towards the foreland (Brun and Faccenna, 2008; Faccenna et al., 2014; Matenco et al., 2016). Our modelling shows that these shifts can result from a combination of lower crustal indentation followed by slab retreat, relamination and eduction (Figs. 2 and 8). This novel explanation for the commonly observed shift between the location of the oceanic suture and the position of the slab detected by teleseismic tomography sheds new light on the geodynamic evolution of these Mediterranean orogens.

5. Conclusions

We investigated numerically an intimate link between the generation of magmatism, and the kinematics, rheology, geometry and tectonic evolution of Mediterranean orogens. These orogens are characterized by slab retreat and the migration of deformation and magmatism towards the orogenic foreland during subduction and subsequent collision. We note that our main results are likely less applicable to other types of orogenic areas, such as the ones associated with large scale plateaus (e.g., the Himalaya-Tibet) or double vergent orogenic wedges (e.g., the Alps or Pyrenees). These are characterized by significantly different deformation and subduction styles, such as lower crustal flow, exhumation in retro-wedges or aligned subduction systems (e.g., Clark and Royden, 2000; Beaumont et al., 2004; Erdős et al., 2014), associated with different mechanisms of magma generation for instance by thickening the upper plate, eclogite root foundering, sub-lithospheric small-scale convections and there is no migration of magmatism and associated geochemistry with time across the orogen (e.g., Ducea et al., 2003; DeCelles et al., 2009; Faccenna and Becker, 2010; Kaislaniemi et al., 2014; Zhengfu Guo et al., 2014).

Our results analysing these specific Mediterranean-type orogens suggest that the rheological and compositional layering of the crust imposes a key control on the distribution of magmatic rocks. We showed that magmatic weakening of the upper plate focuses deformation during subduction and subsequent collision. The influx of more felsic material into the subduction channel during continental subduction creates more crustal magmatic sources that gradually become shallower and continuously migrate towards the foreland. This change focuses deformation at gradually more shallow lithospheric levels and results in the emplacement of progressively more felsic magmatic products. Interestingly, changes in the character of deformation are not necessarily related to a migration of the subduction interface. During oceanic subduction and early collision changes between shortening and extension at far distances from the subduction interface are driven by the magmatic emplacement rather than by the migration of the slab. The formation of a typical subduction-related large-scale magmatic arc is not observed in our models, which would likely require the subduction of larger oceans for longer periods of time. Instead, subduction-related magmatism focusses deformation and results in atypical situations, such as the magmatic emplacement in back-arc extensional (half-) grabens.

During continental collision we observe migration of deformation, movement of the subduction zone and associated magmatism relative to the outcropping location of the former suture zone formed during oceanic subduction. Existing studies generally show that this gradually increasing shift is created by slab retreat (e.g., Doglioni et al., 2007; Duretz and Gerya, 2013). Our results demonstrate an additional component. During early stages of collision the lower crust of the upper plate indents the orogenic wedge, which increases the shift and enables subduction of lower crust. In other words, continental subduction and orogenic build-up are assisted by lower crustal indentation in the overriding plate. This process also explains the migration of magmatism during early stages of collision. At later stages of collision, other processes such as slab detachment may accompany the slab retreat.

Our simulations provide significant new insights for the understanding of the subduction and collision dynamics in the Dinarides. The key characteristics of the Dinarides, such as the foreland propagating deformation and magma front, and the gradual compositional change towards more felsic magmas is explained in our models by lower crustal indentation, relamination and eduction accompanying oceanic and continental subduction. Magmatism in the Timok or Srednogorie grabens that display rather reduced stretching can also be explained by localization of deformation and rheological weakening during magma emplacement and does not necessarily require a period of Late Cretaceous slab retreat. Changes in collisional magmatism observed near the Sava Zone can be explained by a transition to melting in the subduction channel and relamination. We attribute the gradual Oligocene-Miocene transition in the kinematic and magmatic character (from relamination - contraction to eduction - extension) to coeval slab detachment in the Dinarides.

Supplementary data to this article can be found online at https://doi.org/10.1016/j.gr.2017.12.007.

Acknowledgements

This research was financed by the Netherlands Research Centre for Integrated Solid Earth Science (ISES) and the Ministry of Education and Science of the Republic of Serbia (project numbers 176016 and 176019). We gratefully acknowledge the helpful reviews of Mark Allen and Ogus Gogus that have significantly improved the initial manuscript.

References

Andersen, T.B., Jamtveit, B., Dewey, J.F., Swensson, E., 1991. Subduction and eduction of continental crust: major mechanisms during continent-continent collision and orogenic extensional collapse, a model based on the south Norwegian Caledonides. Terra Nova 3, 303–310.

Andrić, N., Sant, K., Matenco, L., Mandic, O., Tomljenović, B., Hrvatović, H., Demir, V., Ooms, J., 2017. The link between tectonics and sedimentation in asymmetric extensional basins: Iinferences from the study of the Sarajevo-Zenica Basin. Marine and Petroleum Geology 83:305–332. https://doi.org/10.1016/j.marpetgeo.2017.02.024.

Balázs, A., Matenco, L., Magyar, I., Horváth, F., Cloetingh, S., 2016. The link between tectonics and sedimentation in back-arc basins: new genetic constraints from the analysis of the Pannonian Basin. Tectonics 35, 1526–1559.

Beaumont, C., Jamieson, R.A., Nguyen, M.H., Medvedev, S., 2004. Crustal channel flows: 1. Numerical models with applications to the tectonics of the Himalayan-Tibetan orogen. Journal of Geophysical Research - Solid Earth 109 (B06406), 1–29.

Beaumont, C., Jamieson, R.A., Butler, J., Warren, C., 2009. Crustal structure: a key constraint on the mechanism of ultra-high-pressure rock exhumation. Earth and Planetary Science Letters 287, 116–129.

Bennett, R.A., Hreinsdóttir, S., Buble, G., Bašić, T., Bačić, Ž., Marjanović, M., Casale, G., Gendaszek, A., Cowan, D., 2008. Eocene to present subduction of southern Adria mantle lithosphere beneath the Dinarides. Geology 36, 3–6.

Brun, J.-P., Faccenna, C., 2008. Exhumation of high-pressure rocks driven by slab rollback. Earth and Planetary Science Letters 272, 1–7.

Burov, E., Yamato, P., 2008. Continental plate collision, P–T–t–z conditions and unstable vs. stable plate dynamics: insights from thermo-mechanical modelling. Lithos 103, 178–204.

Burov, E., Jolivet, L., Le Pourhiet, L., Poliakov, A., 2001. A thermomechanical model of exhumation of high pressure (HP) and ultra-high pressure (UHP) metamorphic rocks in alpine-type collision belts. Tectonophysics 342, 113–136.

Christofides, G., Perugini, D., Koroneos, A., Soldatos, T., Poli, G., Eleftheriadis, G., Del Moro, A., Neiva, A., 2007. Interplay between geochemistry and magma dynamics during magma interaction: an example from the Sithonia Plutonic Complex (NE Greece). Lithos 95, 243–266.

Christofides, G., Krstić, D., Pecskay, Z., 2011. Petrogenesis and tectonic inferences fromthe study of the Mt. Cer pluton (West Serbia). Geological Magazine, Cambridge University Press 148 (1), 89–111.

Clark, M.K., Royden, L.H., 2000. Topographic ooze: building the eastern margin of Tibet by lower crustal flow. Geology 28, 703–706.

Clauser, C., Huenges, E., 1995. Thermal conductivity of rocks and minerals. In: Ahrens, T.J. (Ed.), Rock Physics and Phase Relations. AGU Reference Shelf 3. American Geophysical Union, Washington, DC, pp. 105–126.

Conticelli, S., 1998. The effect of crustal contamination on ultrapotassic magmas with lamproitic affinity: mineralogical, geochemical and isotope data from the Torre Alfina lavas and xenoliths, Central Italy. Chemical Geology 149, 51–81.

Conticelli, S., Avanzinelli, R., Marchionni, S., Tommasini, S., Melluso, L., 2011. Sr-Nd-Pb isotopes from the Radicofani Volcano, Central Italy: constraints on heterogeneities in a veined mantle responsible for the shift from ultrapotassic shoshonite to basaltic andesite magmas in a post-collisional setting. Mineralogy and Petrology 103, 123–148.

Cvetković, V., Prelević, D., Downes, H., Jovanović, M., Vaselli, O., Pécskay, Z., 2004a. Origin and geodynamic significance of Tertiary postcollisional basaltic magmatism in Serbia (central Balkan Peninsula). Lithos 73, 161–186.

Cvetković, V., Downes, H., Prelević, D., Jovanović, M., Lazarov, M., 2004b. Characteristics of the lithospheric mantle beneath East Serbia inferred from ultramafic xenoliths in Palaeogene basanites. Contributions to Mineralogy and Petrology 148, 335–357.

Cvetković, V., Downes, H., Prelević, D., Lazarov, M., Resimić-Šarić, K., 2007a. Geodynamic significance of ultramafic xenoliths from Eastern Serbia: relics of sub-arc oceanic mantle? Journal of Geodynamics 43, 504–527.

Cvetković, V., Poli, G., Christofides, G., Koroneos, A., Pécskay, Z., Resimić-Šarić, K., Erić, V., 2007b. The Miocene granitoid rocks of Mt. Bukulja (central Serbia): evidence for Pannonian extension-related granitoid magmatism in the northern Dinarides. European Journal of Mineralogy 19, 513–532.

Cvetković, V., Downes, H., Höck, V., Prelević, D., Lazarov, M., 2010. Mafic alkaline metasomatism in the lithosphere underneath East Serbia: evidence from the study of xenoliths and the host alkali basalts. Geological Society, London, Special Publications 337, 213–239.

Cvetković, V., Pécskay, Z., Šarić, K., 2013. Cenozoic igneous tectonomagmatic events in the Serbian part of the Balkan Peninsula: inferences from K/Ar geochronology. Acta Volcanologica 10, 111–120.

Davies, J., von Blanckenburg, F., 1995. Slab breakoff: a model of lithosphere detachment and its test in the magmatism and deformation of collisional orogens. Earth and Planetary Science Letters 129, 85–102.

DeCelles, P.G., Ducea, M.N., Kapp, P., Zandt, G., 2009. Cyclicity in Cordilleran orogenic systems. Nature Geoscience 2, 251–257.

Defant, M.J., Drummond, M.S., 1990. Derivation of some modern arc magmas by melting of young subducted lithosphere. Nature 347, 662–665.

Defant, M.J., Jackson, T.E., Drummond, M.S., De Boer, J.Z., Bellon, H., Feigenson, M.D., Maury, R.C., Stewart, R.H., 1992. The geochemistry of young volcanism throughout western Panama and southeastern Costa Rica: an overview. Journal of the Geological Society 149, 569–579.

Dewey, J.F., 1980. Episodicity, sequence and style at convergent plate boundaries. In: Strangway, D.W. (Ed.), The Continental Crust and Its Mineral Deposits. Spec. Pap. 20. Geol. Assoc. of Can., St. John's, Nfld., Canada, pp. 553–573.

Dilek, Y., Altunkaynak, Ş., 2009. Geochemical and temporal evolution of Cenozoic magmatism in western Turkey: mantle response to collision, slab break-off, and lithospheric tearing in an orogenic belt. Geological Society, London, Special Publications 311, 213–233.

Dimitrijević, M.D., 1997. Geology of Yugoslavia. 2nd edition. Geoinstitute, Belgrade, Belgrade (187 pp.).

Doglioni, C., Carminati, E., Cuffaro, M., Scrocca, D., 2007. Subduction kinematics and dynamic constraints. Earth-Science Reviews (ISSN: 0012-8252) 83 (3–4):125–175. https://doi.org/10.1016/j.earscirev.2007.04.001.

Drummond, M., Defant, M., Kepezhinskas, P., 1996. Petrogenesis of slab-derived trondhjemite–tonalite-dacite/adakite magmas. Geological Society of America Special Papers 315, 205–215.

Ducea, M., Lutkov, V., Minaev, V., Hacker, B., Ratschbacher, L., Luffi, P., Schwab, M., Gehrels, G.E., McWilliams, M., Vervoort, J., Metcalf, J., 2003. Building the Pamirs. The view from the underside. Geology 31 (10), 849–852.

Duggen, S., Hoernle, K., van den Bogaard, P., Garbe-Schönberg, D., 2005. Post-collisional transition from subduction-to intraplate-type magmatism in the westernmost Mediterranean: evidence for continental-edge delamination of subcontinental lithosphere. Journal of Petrology 46 (6), 1155–1201.

Duggen, S., Hoernle, K., Klügel, A., Geldmacher, J., Thirlwall, M.F., Hauff, F., Lowry, D., Oates, N., 2008. Geochemistry of Miocene Alborán Basin volcanism, Supplement to: Duggen, S et al. (2008): geochemical zonation of the Miocene Alborán Basin volcanism (westernmost Mediterranean): geodynamic implications. Contributions to Mineralogy and Petrology 156 (5):557–593. https://doi.org/10.1007/s00410-008-0302-4. PANGAEA.

Duretz, T., Gerya, T., 2013. Slab detachment during continental collision: influence of crustal rheology and interaction with lithospheric delamination. Tectonophysics 602, 124–140.

Duretz, T., Gerya, T.V., May, D.A., 2011. Numerical modelling of spontaneous slab breakoff and subsequent topographic response. Tectonophysics 502, 244–256.

Duretz, T., Gerya, T., Kaus, B., Andersen, T., 2012. Thermomechanical modeling of slab eduction. Journal of Geophysical Research - Solid Earth 117.

Dymkova, D., Gerya, T., Burg, J.-P., 2016. 2D thermomechanical modelling of continent–arc–continent collision. Gondwana Research 32, 138–150.

Erak, D., Matenco, L., Toljić, M., Stojadinović, U., Andriessen, P.A.M., Willingshofer, E., Ducea, M.N., 2017. From nappe stacking to extensional detachments at the contact between the Carpathians and Dinarides – The Jastrebac Mountains of Central Serbia. Tectonophysics (ISSN: 0040-1951) 710–711, 162–183.

Erdős, Z., Beek, P., Huismans, R.S., 2014. Evaluating balanced section restoration with thermochronology data: a case study from the Central Pyrenees. Tectonics 33, 617–634.

Faccenda, M., Minelli, G., Gerya, T., 2009. Coupled and decoupled regimes of continental collision: numerical modeling. Earth and Planetary Science Letters 278, 337–349.

Faccenna, C., Becker, T.W., 2010. Shaping mobile belts by small-scale convection. Nature 465, 602–605.

Faccenna, C., Becker, T.W., Conrad, C.P., Husson, L., 2013. Mountain building and mantle dynamics. Tectonics 32, 80–93.

Faccenna, C., Becker, T.W., Auer, L., Billi, A., Boschi, L., Brun, J.P., Capitanio, F.A., Funiciello, F., Horvàth, F., Jolivet, L., 2014. Mantle dynamics in the Mediterranean. Reviews of Geophysics 52, 283–332.

Foley, S., 1992. Vein-plus-wall-rock melting mechanisms in the lithosphere and the origin of potassic alkaline magmas. Lithos 28, 435–453.

Gallhofer, D., Quadt, A.v., Peytcheva, I., Schmid, S.M., Heinrich, C.A., 2015. Tectonic, magmatic, and metallogenic evolution of the Late Cretaceous arc in the Carpathian-Balkan orogen. Tectonics 34, 1813–1836.

Georgiev, N., Henry, B., Jordanova, N., Froitzheim, N., Jordanova, D., Ivanov, Z., Dimov, D., 2009. The emplacement mode of Upper Cretaceous plutons from the southwestern part of the Sredna Gora Zone (Bulgaria): structural and AMS study. Geologica Carpathica 60, 15–33.

Gerya, T., 2010. Dynamical instability produces transform faults at mid-ocean ridges. Science 329, 1047–1050.

Gerya, T.V., Burg, J.-P., 2007. Intrusion of ultramafic magmatic bodies into the continental crust: numerical simulation. Physics of the Earth and Planetary Interiors 160, 124–142.

Gerya, T., Meilick, F., 2011. Geodynamic regimes of subduction under an active margin: effects of rheological weakening by fluids and melts. Journal of Metamorphic Geology 29, 7–31.

Gerya, T.V., Yuen, D.A., 2003a. Characteristics-based marker-in-cell method with conservative finite-differences schemes for modeling geological flows with strongly variable transport properties. Physics of the Earth and Planetary Interiors 140, 293–318.

Gerya, T.V., Yuen, D.A., 2003b. Rayleigh–Taylor instabilities from hydration and melting propel 'cold plumes' at subduction zones. Earth and Planetary Science Letters 212, 47–62.

Gerya, T.V., Stern, R.J., Baes, M., Sobolev, S., Whattam, S.A., 2015. Plate tectonics on the Earth triggered by plume-induced subduction initiation. Nature 527, 221–225.

Göğüş, O.H., Pysklywec, R.N., Faccenna, C., 2016. Postcollisional lithospheric evolution of the Southeast Carpathians: comparison of geodynamical models and observations. Tectonics 35, 1205–1224.

Gray, R., Pysklywec, R.N., 2010. Geodynamic models of Archean continental collision and the formation of mantle lithosphere keels. Geophysical Research Letters 37 (L19301), 1–5.

Guo, Z., Wilson, M., Zhang, L., Zhang, M., Cheng, Z., Liu, J., 2014. The role of subduction channel mélanges and convergent subduction systems in the petrogenesis of post-collisional K-rich mafic magmatism in NW Tibet. Lithos 198, 184–201.

Hacker, B.R., Kelemen, P.B., Behn, M.D., 2011. Differentiation of the continental crust by relamination. Earth and Planetary Science Letters 307, 501–516.

Handy, M.R., M. Schmid, S., Bousquet, R., Kissling, E., Bernoulli, D., 2010. Reconciling plate-tectonic reconstructions of Alpine Tethys with the geological-geophysical record of spreading and subduction in the Alps. Earth-Science Reviews 102, 121–158.

Herak, M., Herak, D., Markušić, S., 1995. Fault plane solutions for earthquakes (1956–1995) in Croatia and neighbouring regions. Geofizika 12, 43–56.

Horváth, F., Cloetingh, S., 1996. Stress-induced late-stage subsidence anomalies in the Pannonian basin. Tectonophysics 266, 287–300.

Jovanović, M., Downes, H., Vaselli, O., Cvetković, V., Prelević, D., Pscskay, Z., 2001. Paleogene mafic alkaline volcanic rocks of East Serbia. Acta Vulcanologica 13, 159–173.

Jull, M., Kelemen, P.B., 2001. On the conditions for lower crustal convective instability. Journal of Geophysical Research - Solid Earth 106, 6423–6446.

Kaislaniemi, L., van Hunen, J., Allen, M.B., Neill, I., 2014. Sublithospheric small-scale convection—a mechanism for collision zone magmatism. Geology 42, 291–294.

Karamata, S., 2006. The geological development of the Balkan Peninsula related to the approach, collision and compression of Gondwanan and Eurasian units. Geological Society, London, Special Publications 260, 155–178.

Kastelic, V., Carafa, M.M.C., 2012. Fault slip rates for the active External Dinarides thrust-and-fold belt. Tectonics 31, TC3019. https://doi.org/10.1029/2011TC003022.

Kelemen, P.B., Behn, M.D., 2016. Formation of lower continental crust by relamination of buoyant arc lavas and plutons. Nature Geoscience 9, 197–205.

Kelemen, P., Hanghøj, K., Greene, A., 2003. One view of the geochemistry of subduction-related magmatic arcs, with an emphasis on primitive andesite and lower crust. Treatise on Geochemistry. vol. 3, pp. 593–659.

Kolb, M., Von Quadt, A., Peytcheva, I., Heinrich, C., Fowler, S., Cvetković, V., 2013. Adakite-like and normal arc magmas: distinct fractionation paths in the East Serbian segment of the Balkan–Carpathian arc. Journal of Petrology 3, 421–451.

Koroneos, A., Poli, G., Cvetković, V., Christofides, G., Krstić, D., Pecskay, Z., 2011. Petrogenesis and tectonic inferences from the study of the Mt. Cer pluton (West Serbia). Geological Magazine, Cambridge University Press 148 (1), 89–111.

Lamb, S., Hoke, L., Kennan, L., Dewey, J., 1997. Cenozoic evolution of the Central Andes in Bolivia and northern Chile. Geological Society, London, Special Publications 121, 237–264.

Liou, J., Zhang, R., Eide, E., Maruyama, S., Wang, X., Ernst, W., 1996. Metamorphism and tectonics of high-P and ultrahigh-P belts in Dabie-Sulu Regions, eastern central China. The Tectonic Evolution of Asia, pp. 300–343.

Lustrino, M., Wilson, M., 2007. The circum-Mediterranean anorogenic Cenozoic igneous province. Earth-Science Reviews 81, 1–65.

Lustrino, M., Duggen, S., Rosenberg, C.L., 2011. The Central-Western Mediterranean: anomalous igneous activity in an anomalous collisional tectonic setting. Earth-Science Reviews 104, 1–40.

Mancktelow, N.S., Stöckli, D.F., Grollimund, B., Müller, W., Fügenschuh, B., Viola, G., Seward, D., Villa, I.M., 2001. The DAV and Periadriatic fault systems in the Eastern Alps south of the Tauern window. International Journal of Earth Sciences 90, 593–622.

Martin, H., 1999. Adakitic magmas: modern analogues of Archaean granitoids. Lithos 46, 411–429.

Matenco, L., Radivojević, D., 2012. On the formation and evolution of the Pannonian Basin: constraints derived from the structure of the junction area between the Carpathians and Dinarides. Tectonics 31, TC6007.

Matenco, L., Krezsek, C., Merten, S., Schmid, S., Cloetingh, S., Andriessen, P., 2010. Characteristics of collisional orogens with low topographic build-up: an example from the Carpathians. Terra Nova 22, 155–165.

Matenco, L., Munteanu, I., Ter Borgh, M., Stanica, A., Tilita, M., Lericolais, G., Dinu, C., Oaie, G., 2016. The interplay between tectonics, sediment dynamics and gateways evolution in the Danube system from the Pannonian Basin to the western Black Sea. Science of the Total Environment 543, 807–827.

Menant, A., Jolivet, L., Vrielynck, B., 2016a. Kinematic reconstructions and magmatic evolution illuminating crustal and mantle dynamics of the eastern Mediterranean region since the late Cretaceous. Tectonophysics 675, 103–140.

Menant, A., Sternai, P., Jolivet, L., Guillou-Frottier, L., Gerya, T., 2016b. 3D numerical modeling of mantle flow, crustal dynamics and magma genesis associated with slab roll-back and tearing: the eastern Mediterranean case. Earth and Planetary Science Letters 442, 93–107.

Naydenov, K., Peytcheva, I., von Quadt, A., Sarov, S., Kolcheva, K., Dimov, D., 2013. The Maritsa strike-slip shear zone between Kostenets and Krichim towns, South Bulgaria—structural, petrographic and isotope geochronology study. Tectonophysics 595, 69–89.

Neill, I., Meliksetian, K., Allen, M.B., Navasardyan, G., Kuiper, K., 2015. Petrogenesis of mafic collision zone magmatism: the Armenian sector of the Turkish–Iranian Plateau. Chemical Geology 403, 24–41.

Ota, T., Terabayashi, M., Parkinson, C.D., Masago, H., 2000. Thermobaric structure of the Kokchetav ultrahigh-pressure–high-pressure massif deduced from a north–south transect in the Kulet and Saldat–Kol regions, northern Kazakhstan. Island Arc 9, 328–357.

Oxburgh, E.R., 1972. Flake tectonics and continental collision. Nature 239, 202–204.

Pamić, J., 2002. The Sava-vardar Zone of the Dinarides and Hellenides versus the Vardar Ocean. Eclogae Geol Helv 95, 99–113.

Peacock, S.M., Keken, P.E.V., Holloway, S.D., Hacker, B.R., Abers, G.A., Fergason, R.L., 2005. Thermal structure of the Costa Rica – Nicaragua subduction zone. Physics of the Earth and Planetary Interiors 149, 187–200.

Pearce, J.A., Bender, J.F., De Long, S.E., Kidd, W.S.F., Low, P.J., Güner, Y., Saroglu, F., Yilmaz, Y., Moorbath, S., Mitchell, J.G., 1990. Genesis of collision volcanism in Eastern Anatolia, Turkey. Journal of Volcanology and Geothermal Research 44, 189–229.

Picotti, V., Pazzaglia, F.J., 2008. A new active tectonic model for the construction of the Northern Apennines mountain front near Bologna (Italy). Journal of Geophysical Research - Solid Earth 113 (B08), 1–24.

Piromallo, C., Morelli, A., 2003. P wave tomography of the mantle under the Alpine-Mediterranean area. Journal of Geophysical Research - Solid Earth 108 (B2), 1–23.

Prelević, D., Foley, S., 2007. Accretion of arc-oceanic lithospheric mantle in the Mediterranean: evidence from extremely high-Mg olivines and Cr-rich spinel inclusions in lamproites. Earth and Planetary Science Letters 256, 120–135.

Prelević, D., Foley, S., Romer, R., Cvetković, V., Downes, H., 2005. Tertiary ultrapotassic volcanism in Serbia: constraints on petrogenesis and mantle source characteristics. Journal of Petrology 46, 1443–1487.

Prelević, D., Jacob, D.E., Foley, S.F., 2013. Recycling plus: a new recipe for the formation of Alpine–Himalayan orogenic mantle lithosphere. Earth and Planetary Science Letters 362, 187–197.

Pysklywec, R.N., Beaumont, C., Fullsack, P., 2002. Lithospheric deformation during the early stages of continental collision: numerical experiments and comparison with South Island, New Zealand. Journal of Geophysical Research - Solid Earth 107 (ETG 3-1–ETG 3-19).

Pysklywec, R.N., Gogus, O., Percival, J., Cruden, A.R., Beaumont, C., 2010. Insights from geodynamical modeling on possible fates of continental mantle lithosphere: collision, removal, and overturn. This article is one of a series of papers published in this Special Issue on the theme Lithoprobe — parameters, processes, and the evolution of a continent. Canadian Journal of Earth Sciences 47, 541–563.

Ranalli, G., 1995. Rheology of the Earth. Chapman and Hall, London, p. 413.

Regenauer-Lieb, K., Yuen, D.A., Branlund, J., 2001. The Initiation of Subduction: Criticality by Addition of Water Science. vol. 294 pp. 578–580.

Royden, L.H., 1993. Evolution of retreating subduction boundaries formed during continental collision. Tectonics 12, 629–638.

Schefer, S., Cvetković, V., Fügenschuh, B., Kounov, A., Ovtcharova, M., Schaltegger, U., Schmid, S.M., 2011. Cenozoic granitoids in the Dinarides of southern Serbia: age of intrusion, isotope geochemistry, exhumation history and significance for the geodynamic evolution of the Balkan peninsula. International Journal of Earth Sciences 100, 1181–1206.

Schmid, S.M., Bernoulli, D., Fügenschuh, B., Matenco, L., Schefer, S., Schuster, R., Tischler, M., Ustaszewski, K., 2008. The Alpine-Carpathian-Dinaridic orogenic system: correlation and evolution of tectonic units. Swiss Journal of Geosciences 101, 139–183.

Seghedi, I., Downes, H., 2011. Geochemistry and tectonic development of Cenozoic magmatism in the Carpathian–Pannonian region. Gondwana Research 20, 655–672.

Seghedi, I., Downes, H., Szakács, A., Mason, P.R., Thirlwall, M.F., Roşu, E., Pécskay, Z., Márton, E., Panaiotu, C., 2004. Neogene–Quaternary magmatism and geodynamics in the Carpathian–Pannonian region: a synthesis. Lithos 72, 117–146.

Sizova, E., Gerya, T., Brown, M., 2012. Exhumation mechanisms of melt-bearing ultrahigh pressure crustal rocks during collision of spontaneously moving plates. Journal of Metamorphic Geology 30, 927–955.

Šoštarić, S.B., Cvetković, V., Neubauer, F., Palinkaš, L.A., Bernroider, M., Genser, J., 2012. Oligocene shoshonitic rocks of the Rogozna Mts.(Central Balkan Peninsula): evidence of petrogenetic links to the formation of Pb–Zn–Ag ore deposits. Lithos 148, 176–195.

Stojadinović, U., Matenco, L., Andriessen, P.A., Toljić, M., Foeken, J.P., 2013. The balance between orogenic building and subsequent extension during the Tertiary evolution of the NE Dinarides: constraints from low-temperature thermochronology. Global and Planetary Change 103, 19–38.

Stojadinović, U., Matenco, L., Andriessen, P., Toljić, M., Rundić, L., Ducea, M.N., 2017. Structure and provenance of Late Cretaceous–Miocene sediments located near the NE Dinarides margin: inferences from kinematics of orogenic building and subsequent extensional collapse. Tectonophyics 710–711, 184–204.

Šumanovac, F., Dudjak, D., 2016. Descending lithosphere slab beneath the Northwest Dinarides from teleseismic tomography. Journal of Geodynamics 102, 171–184.

Tirel, C., Brun, J.P., Burov, E., 2004. Thermomechanical modeling of extensional gneiss domes. In: Whitney, D.L., Teyssier, C., Siddoway, C.S. (Eds.), Gneiss Domes in Orogeny. Geological Society of America Special Paper 380, Boulder, Colorado, pp. 67–78.

Toljić, M., Matenco, L., Ducea, M.N., Stojadinović, U., Milivojević, J., Đerić, N., 2013. The evolution of a key segment in the Europe–Adria collision: the Fruška Gora of northern Serbia. Global and Planetary Change 103, 39–62.

Tomljenović, B., Csontos, L., 2001. Neogene–Quaternary structures in the border zone between Alps, Dinarides and Pannonian Basin (Hrvatsko zagorje and Karlovac Basins, Croatia). International Journal of Earth Sciences 90, 560–578.

Tschegg, C., Ntaflos, T., Seghedi, I., Harangi, S., Kosler, J., Coltorti, M., 2010. Paleogene alkaline magmatism in the South Carpathians (Poiana Ruscă, Romania): Asthenospheric melts with geodynamic and lithospheric information. Lithos 120, 393–406.

Turcotte, D.L., Schubert, G., 1982. Geodynamics: Application of Continuum Physics toGeological Problems. John Wiley, New York.

Turcotte, D., Schubert, G., 2002. Geodynamics. Cambridge Univ. Press, Cambridge, UK (doi 10.0521666244. 472 pp.).

Ueda, K., Gerya, T.V., Burg, J.P., 2012. Delamination in collisional orogens: thermomechanical modeling. Journal of Geophysical Research - Solid Earth 117.

Ustaszewski, K., Kounov, A., Schmid, S.M., Schaltegger, U., Krenn, E., Frank, W., Fügenschuh, B., 2010. Evolution of the Adria-Europe plate boundary in the northern Dinarides: from continent-continent collision to back-arc extension. Tectonics 29, TC6017. https://doi.org/10.1029/2010TC002668.

Uyeda, S., Kanamori, H., 1979. Back-arc opening and the mode of subduction. Journal of Geophysical Research - Solid Earth 84, 1049–1061.

Vergés, J., Fernàndez, M., 2012. Tethys–Atlantic interaction along the Iberia–Africa plate boundary: the Betic–Rif orogenic system. Tectonophysics 579, 144–172.

Vissers, R.L.M., Meijer, P.T., 2012. Iberian plate kinematics and Alpine collision in the Pyrenees. Earth-Science Reviews 114, 61–83.

Vogt, K., Gerya, T.V., Castro, A., 2012. Crustal growth at active continental margins: numerical modeling. Physics of the Earth and Planetary Interiors 192, 1–20.

Vogt, K., Matenco, L., Cloetingh, S., 2017a. Crustal mechanics control the geometry of mountain belts. Insights from numerical modelling. Earth and Planetary Science Letters 460, 12–21.

Vogt, K., Willingshofer, E., Matenco, L., Sokoutis, D., Gerya, T., Cloetingh, S., 2017b. The role of lateral strength contrasts in orogenesis: a 2D numerical study. Tectonophysics https://doi.org/10.1016/j.tecto.2017.08.010.

von Quadt, A., Peytcheva, I., 2005. The southern extension of the Srednogorie type Upper Cretaceous magmatism in Rila-Western Rhodopes: Constraints from isotope geochronological and geochemical data, paper presented at 80 years. Bulgarian Geological Society, Bulgarian Geol. Soc., Sofia, Bulgaria.

von Quadt, A., Peytcheva, I., Kamenov, B., Fanger, L., Heinrich, C.A., Frank, M., 2002. The Elatsite porphyry copper deposit in the Panagyurishte ore district, Srednogorie zone, Bulgaria: U-Pb zircon geochronology and isotope-geochemical investigations of magmatismand ore genesis. In: Blundell, D.J., Neubauer, F., von Quadt, A. (Eds.), Timing and Location of Major Ore Deposits in an Evolving Orogen. Geol. Soc., London, pp. 119–135.

von Quadt, A., Peytcheva, I., Cvetkovic, V., 2003. Geochronology, geochemistry and isotope tracing of the Cretaceous magmatism of East-Serbia and Panagyurishte district (Bulgaria) as part of the Apuseni–Timok–Srednogorie metallogenic belt in Eastern Europe. Mineral Exploration and Sustainable Development. Mill press, Rotterdam, pp. 407–410.

Willingshofer, E., Sokoutis, D., 2009. Decoupling along plate boundaries: key variable controlling the mode of deformation and the geometry of collisional mountain belts. Geology 37, 39–42.

Willingshofer, E., Sokoutis, D., Luth, S., Beekman, F., Cloetingh, S., 2013. Subduction and deformation of the continental lithosphere in response to plate and crust-mantle coupling. Geology 41, 1239–1242.

Zelić, M., Agostini, S., Marroni, M., Pandolfi, L., Tonarini, S., 2010. Geological and geochemical features of the Kopaonik intrusive complex (Vardar zone, Serbia). Ofioliti 35 (1), 33–47.